Discoidin domain receptor regulates ensheathment, survival, and caliber of peripheral axons

Megan M. Corty[1], Alexandria P. Lassetter[1], Jo Q. Hill[2], Amy E. Sheehan[1], F. Javier Bernardo-Garcia[2], Graeme W. Davis[2], Sue A. Aicher[3], Marc R. Freeman[1]

[1]Vollum Institute, Oregon Health & Science University, Portland, OR, 97239, USA

[2] Department of Biochemistry and Biophysics, Kavli Institute for Fundamental Neuroscience, University of California, San Francisco, San Francisco, CA 94158, USA

[3]Department of Chemical Physiology & Biochemistry, Oregon Health & Science University, 97239, Portland, OR, USA

Correspondence: freemmar@ohsu.edu

Key Words: wrapping glia, *Drosophila*, Remak Schwann cell, Multiplexin, axon ensheathment

Abstract

Invertebrate axons and small caliber axons in mammalian peripheral nerves are unmyelinated but still ensheathed by glia. How this type of ensheathment is controlled and its roles in supporting neuronal function remain unclear. We performed an *in vivo* RNAi screen in *Drosophila* to identify glial genes required for axon ensheathment and identified the conserved receptor tyrosine kinase Discoidin domain receptor (Ddr). In larval peripheral nerves, loss of Ddr resulted in incomplete ensheathment of axons. We found a strong dominant genetic interaction between *Ddr* and the fly type XV/XVIII collagen *Multiplexin (Mp)*, suggesting Ddr functions a collagen receptor to drive wrapping of axons during development. Surprisingly, while ablation of glia that wrap axons severely impaired larval motor behavior, incomplete wrapping in *Ddr* mutants was sufficient to support basic circuit function. In adult nerves, loss of Ddr from glia decreased long-term survival of sensory neurons and significantly reduced axon caliber without overtly affecting ensheathment. Our data establish a crucial role for non-myelinating glia in peripheral nerve development and function across the lifespan, and identify Ddr as a key regulator of axon-glia interactions during ensheathment.

Introduction

In complex nervous systems, specialized glial cells ensheathe long axons, and this wrapping can take many forms. Myelination is the most studied type of ensheathment, but unmyelinated axons make up the majority (~70%) of axons in human peripheral nerves (Ochoa and Mair, 1969; Schmalbruch, 1986). Vertebrate Remak Schwann cells ensheathe and separate unmyelinated axons from one another. These small caliber axons include many types of sensory

neuron axons, including nociceptive c-fibers and autonomic axons (Griffin and Thompson, 2008). Remak Schwann cells are positioned to mediate fundamental aspects of nerve development and sensory biology, and be important modulators of neurological conditions affecting the peripheral nervous system (PNS) including peripheral neuropathies and nerve injuries. However, Remak Schwann cells have remained understudied, in part due to a lack of selective genetic tools to specifically target this population.

In *Drosophila,* axons in peripheral nerves are ensheathed by specialized wrapping glia in a manner analogous to vertebrate Remak bundles (Figure 1A-B). *Drosophila* larval abdominal nerves project out of the ventral nerve cord in each segment and contain both motor and sensory neuron axons surrounded by multiple glial layers: the outermost perineurial glia, then subperineural glia, and finally axon-associated wrapping glia (Hilchen et al., 2013; Matzat et al., 2015; Stork et al., 2008)(Figure 1A,B). Wrapping is progressive throughout larval life. In embryos, axons are initially tightly fasciculated without intervening glial processes. Wrapping progresses such that by third instar axons are wrapped either individually or in small bundles by wrapping glia membrane (Figure 1B, C) (Matzat et al., 2015). This process mirrors vertebrate nerve development when Schwann cells perform radial sorting of axons that are initially tightly fasciculated (Monk et al., 2015) and a growing body of evidence that demonstrates a high degree of cellular and molecular conservation between ensheathment mechanisms in *Drosophila* and vertebrates (Ghosh et al., 2013; Matzat et al., 2015; Mukherjee et al., 2020; Petley-Ragan et al., 2016; Xie and Auld, 2011). This Remak-like type of multi-axonal ensheathment is thought to represent an ancient form of axon-glial association, and the emerging cellular and molecular conservation of multiple aspects of peripheral nerve biology make *Drosophila* wrapping glia a promising model to study non-myelinating ensheathment *in vivo*.

Beyond simply insulating individual axons, glia that ensheathe axons also regulate neuronal development, maintenance, and function throughout an animal's lifespan. Myelination can alter the distribution of axonal proteins, increase axon caliber, and is important for trophic and metabolic support of long axons, though the precise mechanisms by which myelinating glia perform all of these functions remain incompletely understood (Nave, 2010). Recent work supports the notion that Remak Schwann cells play similar important roles: perturbation of Schwann cell metabolism results in axon degeneration, with small caliber, Remak-ensheathed axons degenerating earlier than myelinated ones (Beirowski et al., 2014). Although Remak Schwann cells were not targeted selectively, these observations support the notion that unmyelinated axons are also reliant on glial support.

Here we take advantage of *Drosophila* wrapping glia as a model to identify new molecular regulators of glial ensheathment and support of axons. Through an RNAi-based screen, we identify *Discoidin domain receptor* (*Ddr*) as crucial for glial ensheathment in larval nerves. We demonstrate that wrapping glia are essential for normal nerve function and behavior by developing a new Split-Gal4 intersectional driver to genetically ablate larval wrapping glia, which results in severely impaired crawling behavior. Surprisingly, while loss of Ddr results in incomplete wrapping, it did not result in overt effects on behavior, arguing that even partial ensheathment is sufficient to support normal nerve function. In adult nerves, loss of *Ddr* results in reduced long-term survival of peripheral sensory neurons and reduced axon caliber without affecting ensheathment. Ddr is therefore a new glial regulator of axon caliber *in vivo*. Finally, we identify the collagen multiplexin (Mp) as a potential ligand for Ddr in driving wrapping during development, suggesting that Ddr-collagen interactions are critical regulators of axon ensheathment and glial support of neurons.

FIGURE 1

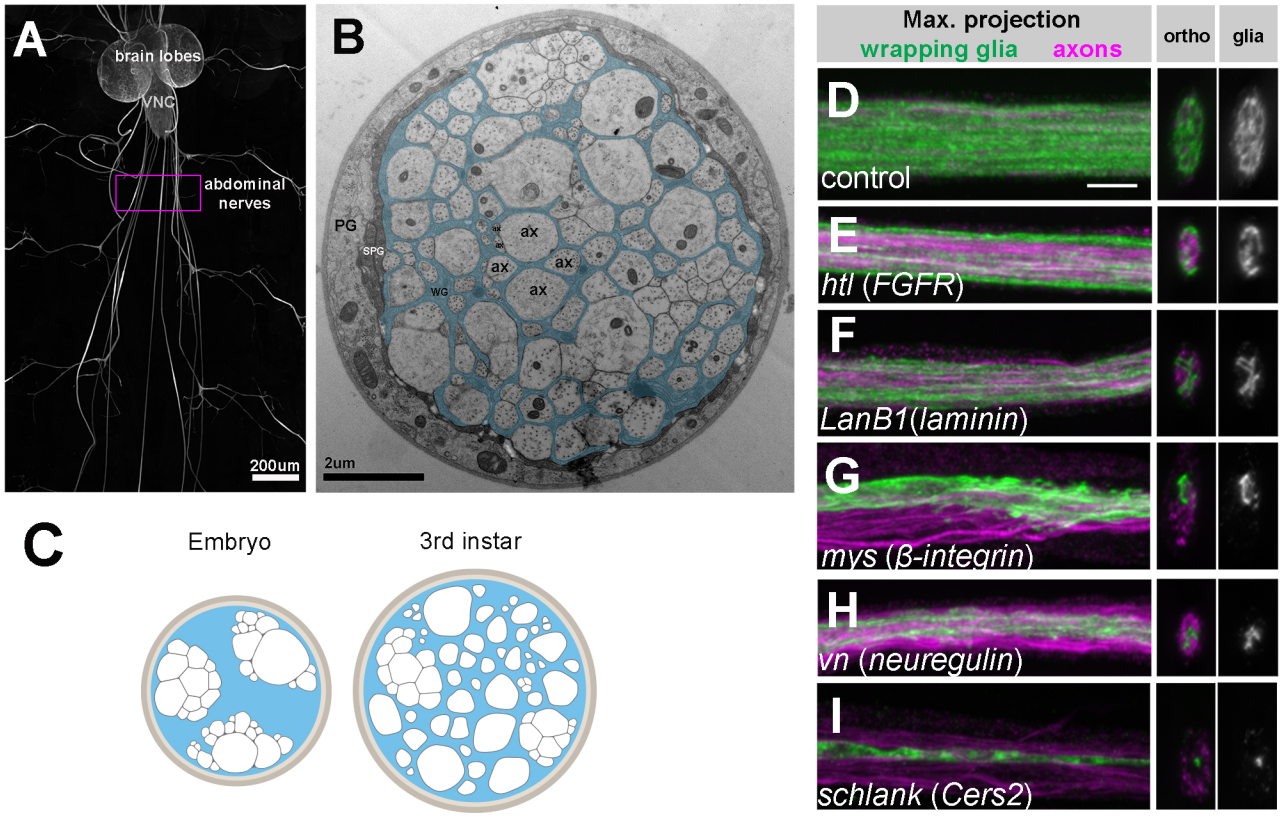

Figure 1: *Drosophila* wrapping glia are a model of multi-axonal ensheathment

(A) Confocal image showing a 3rd instar larval nervous system including the brain, ventral nerve cord (VNC), and peripheral nerves as labeled in a *nrv2-Gal4>UASmCD8:GFP* animal. This driver labels wrapping glia in the nerves as well as some subtypes of CNS glia in the brain and VNC. Boxed region corresponds to the approximate area imaged for glial morphology analysis. **(B)** TEM cross-section of a third instar larval nerve. Light, round profiles of larval axons (ax) are surrounded by darker (pseudo-colored cyan) wrapping glia. Subperineurial (SPG) and perineurial glia (PG; not colored) form the outer layers of the nerve, which is coated by a neural lamella of ECM proteins. **(C)** Schematic representation of larval nerve cross sections at hatching and 3rd instar stages illustrating that wrapping is progressive over larval development. **(D-H)** RNAi against genes with known roles in wrapping glia and vertebrate glia development results in visible morphological defects at the light level. Wrapping glia are labeled with myr:tdTomato driven by *nrv2-Gal4* (pseudo-colored green). A subset of sensory axons are labeled with anti-Futsch (magenta). A maximum confocal projection of the nerve is shown in the left panel. The ortho panel shows the nerve cross section, and the glia channel is the isolated wrapping glial channel in cross section. Scale bar 5µm. **(D)** Control nerves show fairly uniform, honeycomb-like glia membrane coverage of the nerve cross section. **(E)**Wrapping glial knockdown of *heartless*, an FGF Receptor homolog, shows incomplete glial coverage of the nerve cross section. **(F)** Knockdown of *lanB1*, a laminin homolog, causes impaired cross section coverage. **(G)** Knockdown of the β-integrin homolog *myospheroid* causes highly abnormal glia morphology where glia fail to cover the entire nerve. **(H)** Knockdown of the neuregulin homolog, *vein*, results in impaired glia coverage of the nerve cross section. **(I)** Knockdown of *schlank*, a Ceramide Synthetase-2 homolog, results in thin stringy glia that does not appear to wrap axons at all.

RESULTS

Morphology based RNAi screen identifies *Ddr* as a regulator of wrapping glia development

To identify genes that are required in glia for normal ensheathment of axons, we conducted a morphology based RNAi screen to systematically knock down genes in wrapping glia and look for changes in glial morphology in third instar larval nerves (Matzat et al. 2015; Stork et al. 2008). To visualize and manipulate wrapping glia, we used the well-established *nrv2-Gal4* driver line which, within the PNS, is strongly and exclusively expressed in wrapping glia (Stork et al., 2008; Xie and Auld, 2011). We expressed a membrane bound marker (*UAS-myr:tdTomato*) to visualize wrapping glia morphology and *UAS-RNAi* constructs from the Vienna *Drosophila* Resource Collection to knock down genes selectively in wrapping glia throughout development. In total, we screened a collection of ~2000 RNAi lines, which comprise the majority of transmembrane, secreted, and signaling proteins in the fly genome and included the fly homologs of ~200 genes strongly expressed in the developing mouse oligodendrocyte lineage based on available RNA-seq data (Zhang et al., 2014).

Using spinning disk confocal microscopy and examination of nerve cross sections, we found that wild type wrapping glia morphology in third instar larvae includes membrane coverage throughout the interior of the nerve with small, regularly spaced gaps like a tight honeycomb (Figure 1D and Figure 2—figure supplement 1A,B). As a positive control for our screen, we knocked down genes previously shown to be involved in wrapping glia development including the neuregulin homolog *vein*, the FGF receptor *heartless*, integrin receptors, laminin, and the ceramide synthetase gene, *schlank* (Franzdóttir et al., 2009; Ghosh et al., 2013; Kottmeier et al., 2020; Matzat et al., 2015; Petley-Ragan et al., 2016; Xie and Auld, 2011), all of

105 which resulted in easily identifiable defects in axon ensheathment using confocal microscopy
106 (Figure 1E-I). Each of these genes have homologs that have been implicated in oligodendrocyte
107 and/or Schwann cell development, further arguing for strong molecular conservation among both
108 vertebrate and invertebrate axonal ensheathment mechanisms (Barros et al., 2009; Feltri et al.,
109 2002; Furusho et al., 2009; Lyons et al., 2005; Michailov et al., 2004; Pereira et al., 2009;
110 Stassart et al., 2013; Taveggia et al., 2005; Yu et al., 2009).

111 Among potential hits whose function had not previously been studied in either vertebrate
112 or invertebrate glia was the *Discoidin domain receptor* (*Ddr*) gene (Figure 2A). Knocking down
113 *Ddr* using two independent RNAi constructs led to altered wrapping glia morphology with the
114 nerve cross section incompletely covered by glial membrane, suggesting that axons were not
115 properly wrapped when *Ddr* was knocked down (Figure 2B-D). *Drosophila Ddr* encodes a
116 receptor tyrosine kinase homologous to vertebrate Ddr1 and Ddr2. In the mouse, Ddr1 is
117 expressed in Schwann cells and the oligodendrocyte lineage (Franco-Pons et al., 2006; Gerber et
118 al., 2021; Roig et al., 2010; Zhang et al., 2014), but direct roles for Ddr1in regulating
119 ensheathment of axons have not been reported. Thus, the results from our screen provide the
120 first functional indication that this receptor could be involved in regulating axonal wrapping.
121
122 **_Ddr_ mutants exhibit defects in axonal ensheathment**
123 To confirm that *Ddr* is involved in wrapping glia development, we created mutant alleles
124 of *Ddr* using a CRISPR-Cas9 strategy. Briefly, using two gRNAs against widely spaced,
125 adjacent exons, we generated fly stocks in which an ~11kb region of the *Ddr* coding region was
126 excised near the 5' end (Figure 2A & 2H). We sequenced the resulting deletion lines to identify
127 mutants that resulted in frame shift mutations and early stop codons. *Ddr* encodes two potential

FIGURE 2

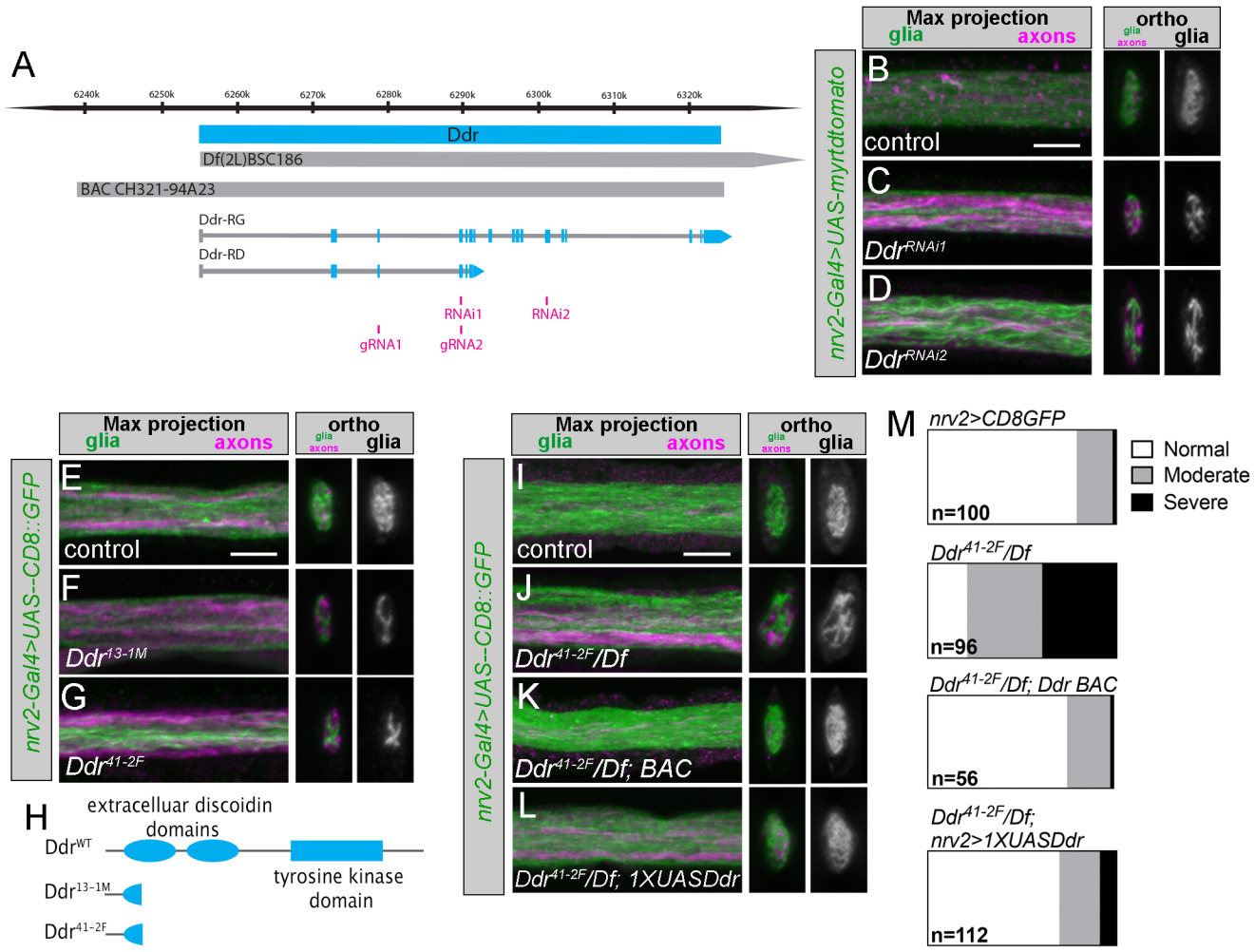

Figure 2: Ddr is required for normal wrapping glia morphogenesis

(A) Model of the *Ddr* genetic locus showing the coding region (cyan); the deficiency used in experiments: *Df(2L)BSC186*; the region that the rescue BAC covers; the location of the RNAi target regions (magenta); and locations of the guide RNAs used for the CRISPR-mediated mutagenesis (magenta). **(B-D)** Representative images of Ddr RNAi knockdown with 2 independent RNAi constructs. *Nrv2-Gal4* driven tdTomato is pseudocolored green. A subset of axons is labeled with anti-Futsch antibody (magenta). Compared to control nerves **(B)**, RNAi conditions show large patches of the nerve cross section without glia membrane coverage **(C,D)**. **(E-G)** Representative images of *Ddr* homozygous mutant experiments. Compared to control **(E)** both CRISPR mutant alleles show severe defective glia coverage in the nerve cross sections **(F-G)**. **(H)** Ddr is a transmembrane receptor tyrosine kinase characterized by extracellular discoidin and discoidin-like domains and an intracellular tyrosine kinase domain. The mutant alleles generated by CRISPR-CAS9 result in a severely truncated peptide without any full domains. **(I-L)** Representative images of *Ddr* loss of function experiments. **(I)** *Nrv2-Gal4, UAS-CD8:GFP/+* was used to visualize glial morphology and is in the background of all conditions. **(J)** *Ddr^{41-2F}/DfBSC186 ("Ddr* mutant*")* nerves show incomplete coverage of the nerve cross section. This example shows a "moderate" phenotype, more examples of moderate and severe phenotypes can be seen in Supplemental Figure S2A. **(K)** Introduction of a BAC transgene to resupply endogenous *Ddr* expression largely restores normal morphology. **(L)** Expression of a *1xUAS-Ddr* construct in wrapping glia using *Nrv2-Gal4* similarly restores normal morphology. **(M)** Categorical scoring of nerve wrapping glia phenotypes. n= # of nerves scored (8-14 larvae per condition). Scale bars = 5μm.

isoforms: a short isoform that is 380 amino acids and lacks both transmembrane and kinase domains, and a full-length isoform that encodes a 1054 amino acid protein. We identified two independent alleles that are predicted nulls, as they result in 150 amino acid ($Ddr^{13\text{-}1M}$) or 134 amino acid ($Ddr^{41\text{-}2F}$) long peptides lacking all known functional domains (Figure 2H). Both mutant alleles were homozygous viable and viable when placed in *trans* to large deficiencies that uncover the *Ddr* coding region. We analyzed the nerves of *Ddr* homozygous mutant animals using florescent confocal microscopy and found that wrapping glia morphology was impaired as we had observed in the wrapping glia-specific RNAi knockdown experiments (Figure 2E-G). We focused our loss of function analyses on using the combination of $Ddr^{41\text{-}2F}$ and *Df(2L) BSC186*, the shortest deficiency that still deletes the entire *Ddr* coding region (Figure 2A). We found that animals lacking any functional Ddr had impaired wrapping (Figure 2I-J, 2M; control: 79% normal morphology; *Ddr/Df*: 21% normal morphology; see Figure 2—figure supplement 1 for examples of categorical scoring). Introduction of a single copy of a BAC clone containing the entire *Ddr* locus and a ~17.4kb upstream region into the mutant strain largely restored normal wrapping morphology (Figure 2K, 2M; BAC rescue: 75% normal morphology), as did resupplying Ddr in wrapping glia via a *1xUAS-Ddr* construct driven by *nrv2-Gal4* (Figure 2L, 2M; *1xUAS* rescue: 70% normal morphology). Higher level overexpression using a *5xUAS-Ddr* construct caused morphological defects in a control background that the *1xUAS-Ddr* construct did not, suggesting that Ddr levels may need to be tightly regulated to promote normal wrapping and morphological development (Figure 2—figure supplement 2). Together these results confirmed our RNAi results that Ddr is required cell autonomously in wrapping glia to regulate axon ensheathment.

While data from fluorescent images supported the notion that significant ensheathment defects resulted from loss of Ddr, we wanted to quantify more precisely how wrapping was affected in Ddr mutants. We therefore analyzed nerves from control and *Ddr* mutant animals using transmission electron microscopy (TEM) and used the "wrapping index" (WI) metric to quantify ensheathment defects (Matzat et al., 2015). WI is equal to the number of individually wrapped axons plus the number of small bundles of axons, divided by the total number of axonal profiles and is expressed as a percentage. In control condition nerves, wrapping glia membrane separated axons in small bundles or individually (Figure 3A-B). The average WI in control conditions was ~21% (Figure 3F: *nrv2* driver control: mean= 22.5%, n=26 nerves from 5 larvae, w^{1118} control: mean= 21%, n=15 nerves from 3 larvae), consistent with previous reports (Matzat et al., 2015). We observed less separation of axons by wrapping glia membrane in Ddr conditions (Figure 3C-D), and this was reflected in both $Ddr^{\Delta 1-2F}$ homozygous and $Ddr^{\Delta 1-2F}$/*Df(2L)BSC186* conditions showing a significant decrease in wrapping index (Figure 3F: *Ddr/Ddr* mean=14.8%, n=30 nerves from 4 larvae, p=0.0006 compared to *nrv2* control; *Ddr/Df(2L)BSC186*: mean= 11.9%, n=33 nerves from 4 larvae, p<0.0001 compared to *nrv2* control, one-way ANOVA with Dunnett's multiple comparisons). These data confirm that loss of Ddr impairs axonal wrapping during development.

To determine whether loss of Ddr specifically affected wrapping glia or more grossly disrupted the morphology of the nerve, we also assessed the other glial and axonal populations within the nerves of Ddr mutants. We did not observe any changes in either subperineurial or perineurial glia in TEM sections in the mutant conditions, nor differences in the total number of axon profiles observed (Figure 3—figure supplement 1), suggesting that overall nerve assembly

FIGURE 3

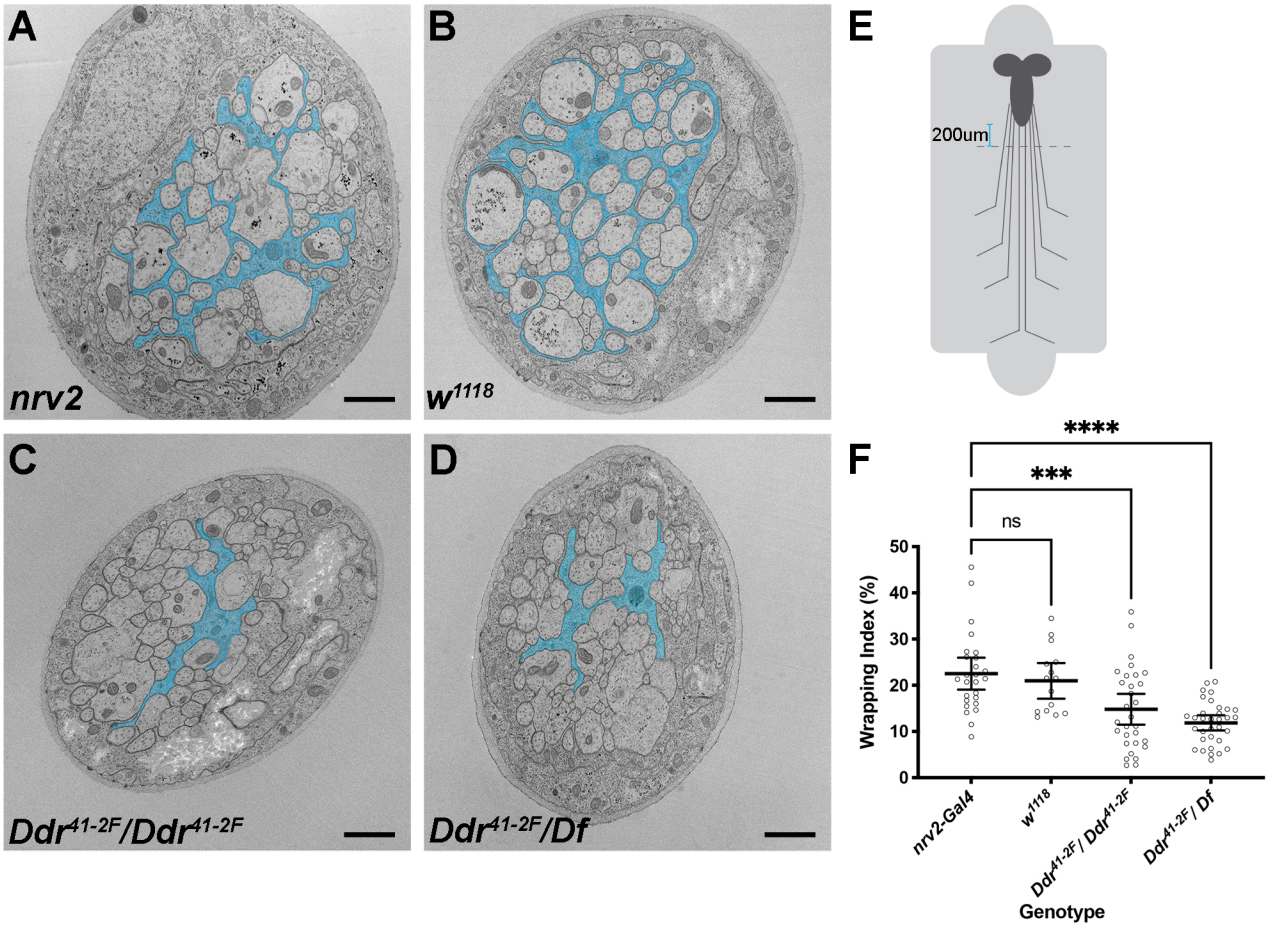

Figure 3: Loss of *Ddr* impairs axon ensheathment in larval nerves

(A) TEM cross section of an abdominal nerve from a control *nrv2-Gal4, UAS-CD8:GFP/+* 3rd instar larvae. Wrapping glia membrane is pseudocolored cyan. **(B)** TEM cross section of an abdominal nerve from a control w^{1118} 3rd instar larva. **(C)** TEM cross section of an abdominal nerve from a $Ddr^{41\text{-}2F}$ homozygous mutant animal ($Ddr^{41\text{-}2F}$/ $Ddr^{41\text{-}2F}$; *nrv2-Gal4, UAS-CD8:GFP/+*). **(D)** TEM cross section of an abdominal nerve from a *Ddr* loss of function animal ($Ddr^{41\text{-}2F}$*/Df(2L)BSC186; nrv2-Gal, UAS-CD8:GFP/+*). **(E)** Schematic of larval fillets prepped for TEM. Sections for analysis are collected ~200um from the distal tip of the VNC. **(F)** Quantification using the wrapping index (WI) metric. Wrapping index was reduced in Ddr loss of function conditions compared to control conditions in larval nerves. *Nrv2-Gal4, UAS-mCD8:GFP/+* controls (WI: 22.5%, n= 26 nerves, 5 larvae); w^{1118} wildtype background strain (WI: 21%, n=15 nerves, 3 larvae, p=0.9546); $Ddr^{-/-}$ (WI: 14.8%, n= 30 nerves, 4 larvae, p=0.0006); *Ddr/Df* (WI: 11.9%,n=33 nerves, 4 larvae, p<0.0001); One-way ANOVA with Dunnett's multiple comparisons against *Nrv2-Gal4*. Error bars: 95% Confidence interval. Scale bars = 1μm

was relatively normal. Therefore loss of Ddr seems to specifically alter wrapping without disrupting nerve morphology.

Incomplete ensheathment of axons is not sufficient to alter crawling behaviors

We next sought to determine whether a decrease in multi-axonal ensheathment might impact neuronal health and function. Larval nerves are mixed nerves that contain both the motor and sensory axons that together mediate larval crawling behavior. To see if basic locomotion was affected when normal axonal ensheathment was impaired, we assayed larval crawling behavior in *Ddr* mutant third instar larvae by monitoring crawling on a non-nutritive agar surface using the FIMTracker system (Risse et al., 2017). Comparing overall distance travelled over a one minute period, we did not see any significant effects on basic crawling behavior between control and *Ddr* mutant larvae (Figure 4A-B). One interpretation of these results is that wrapping is completely dispensable, at least for basic crawling behaviors. Alternatively, it is possible that even the incomplete wrapping observed in *Ddr* mutants is sufficient to support neuronal function and this basic behavior over the ~5 day period of larval life.

Genetic ablation of wrapping glia impairs larval crawling

To further distinguish between these possibilities, we sought to ablate wrapping glia entirely. These experiments required a Gal4 driver that would selectively drive expression exclusively in wrapping glia. Although *Nrv2-gal4* is specific to wrapping glia in the PNS, it does drive expression in some subtypes of CNS glia which would complicate the interpretation of any functional ablation experiments. To generate a clean wrapping glia specific driver line, we turned to a Split-Gal4 intersectional strategy (Luan et al., 2006). First, we created a *nrv2-Gal4*^{DBD}

FIGURE 4

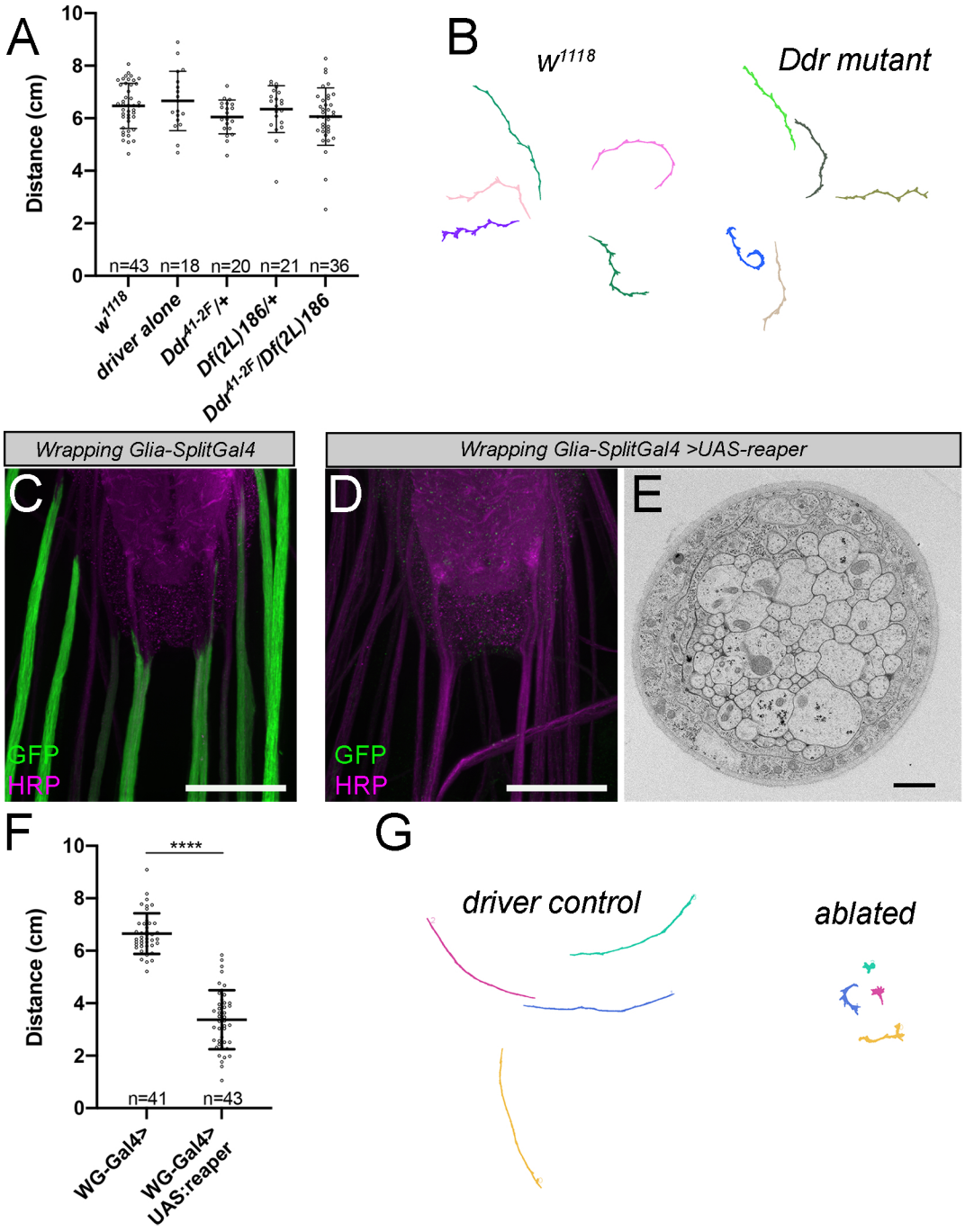

Figure 4: Genetic ablation of wrapping glia impairs larval crawling behavior.
(A) Larval crawling, as measured by distance travelled per minute is not impaired in *Ddr* mutant animals compared to control conditions. One-way ANOVA with Tukey's multiple comparisons, no significant differences between any conditions. n = # of larvae/condition. **(B)** Representative crawling paths from control and *Ddr* mutant larvae. **(C)** Expression pattern of *WG-Split-Gal4* driving *UAS-CD8:GFP* (green). Magenta is an HRP counterstain which labels neuronal membranes. Scale bar, 50µm. **(D)** Representative image of a 3rd instar larvae in which wrapping glia have been genetically ablated. Note the lack of GFP staining along the nerves. Scale bar 50µm. **(E)** TEM image of a nerve cross section from a larva whose wrapping glia has been ablated. All of the axons remain in contact with each other without intervening glial membrane. Scale bar 1µm **(F)** Larval crawling behavior is impaired when wrapping glia are ablated. Unpaired t-test, $p<0.0001$. n = # of larvae/condition. **(G)** Representative crawling paths of control and ablated larvae. The paths from the ablated larvae are shorter and show increased turning, stalling, and reversals. Error bars: standard deviation

construct. This line is capable of driving expression of the DNA binding domain of GAL4 in wrapping glia, cortex glia, ensheathing glia, and astrocytes (Coutinho-Budd et al., 2017). We then identified a line from the InSite collection (*InSite0117-Gal4*) that robustly labeled wrapping glia and a subset of neurons (Figure 4—figure supplement 1). We converted *Insite0117-Gal4* to *Insite0117-GAL4*^{VP16AD} line using the InSite method to swap the domains via genetic crosses (Gohl et al., 2011). In conjunction with *Nrv2-Gal4*^{DBD} this results in specific expression of UAS-transgenes only where the 2 hemi-drivers' expression overlaps—in wrapping glia. No other glia or neurons were observed in the expression pattern (Figure 4C and Figure 4—figure supplement 1). This combination of *nrv2-Gal4*^{DBD} and *IT.0117-Gal4*^{VP16AD} is referred to as *wrapping glia-Split Gal4* (*WG-SplitGal4*).

We used *WG-SplitGal4* to drive expression of *UAS-mCD8:GFP* and *UAS-reaper* to ablate wrapping glia. We observed nearly complete loss of larval wrapping glia cells in resulting progeny based on loss of both fluorescence and an independent wrapping glia nuclear marker that we had identified in the lab, Oaz (Figure 4D and Figure 4—figure supplements 2 and 3). To further confirm the ablation of wrapping glia, we examined the ultrastructure of nerves where wrapping glia were ablated. We saw tightly fasciculated axons without intervening glial membranes confirming that wrapping glia had been eliminated (Figure 4E). Only in a few nerves did we identify anything that might be remnants of wrapping glia. We did not observe any obvious ingrowth of the outer subperineurial or perineurial glia layers to potentially compensate for the loss of wrapping glia and ensheathe axons. However, we did note that several nerves showed an abnormal hypertrophy of the outer perineurial glia layer (Figure 4—figure supplement 3). Surprisingly, when we counted the number of axon profiles in each nerve, we found fewer axonal profiles than the expected ~78 of A3-A7 nerves (w^{1118} average= 77.4 axons;

WG-ablated average= 63 axons; Unpaired t-test p=0.0006), indicating that axons (or entire neurons) might have died or not developed properly as a result of acute wrapping glia loss (Figure 4—figure supplement 3).

Using these tools, we then assayed for defects in crawling behavior and found that animals with ablated wrapping glia crawled significantly less than control animals (Figure 4F-G; mean distance travelled: driver control = 6.65±0.77cm, n=41 larvae, ablated = 3.37±1.126cm, n=43; $p<0.0001$ unpaired t-test). In performing the experiments, we also observed that larvae lacking wrapping glia had difficulty righting themselves when placed on their dorsal sides, and were observed to have abnormal postures and body bends, indicating a possible disruption of bilateral or intersegmental coordination caused by wrapping glia ablation. Together, these data demonstrate that wrapping glia are required in nerves for normal circuit function.

Ensheathment of axons in an adult nerve is not impaired in *Ddr* mutants

Unlike ablation of wrapping glia, incomplete wrapping caused by the loss of Ddr did not significantly affect behavior or neuronal survival during the short larval period (~5 days). However, since neuronal defects that are secondary to glial dysfunction can be age- or stress-related in vertebrate animals (Beirowski et al., 2014; Lappe-Siefke et al., 2003; Saab et al., 2016; Yin et al., 1998; Zöller et al., 2008), we investigated whether Ddr and proper wrapping were required for longer term support of axon health and function. Because the larval period is short and defined, we turned our attention to an accessible adult peripheral nerve, the L1 sensory nerve in the adult wing.

Sensory bristles and campaniform sensilla along the wing's edge are innervated by peripheral sensory neurons located within the L1 wing vein. The axons of these neurons form the

L1 sensory nerve that projects into the thorax (Figure 5A). The organization of the nerve is reported to be similar to larval nerves, with axons ensheathed by wrapping glia (Neukomm et al., 2014). We developed a protocol to perform TEM on the adult wing to examine cross sections of the nerve. By imaging in the region distal to the fusing of the L3 nerve but proximal to the first sensory cell body along the anterior wing margin, we could reliably visualize all of the axons present in the L1 nerve (Figure 5A, dashed red box). In control nerves at 5 dpe, we were surprised to find that all axons appear to be completely separated from one another (Figure 5B), instead of persisting in tightly compacted small bundles as are observed in the larval nerves (compare to Figure 1B). When we examined *Ddr* mutant wings of the same age, we found no obvious defects in wrapping and axon separation between control and *Ddr* mutant wing nerves (Figure 5C-D), in contrast to the impaired wrapping we observed in *Ddr* mutant larval nerves. These data show that wrapping in the adult is more extensive than in larval nerves and seems to be completed during pupal stages or shortly after eclosion. Despite being more extensive and complete, wrapping in adult nerves does not strictly require Ddr. Ddr may be dispensable for wrapping in the adult, work redundantly with other molecules, or cause only a transient delay in wrapping that is rectified within a few days of eclosion.

Loss of Ddr impairs the long-term survival of adult sensory neurons

Despite having no obvious defects in axonal ensheathment, based on our observation of apparent neuronal loss in wrapping glia-ablated larvae, we wondered whether long-term neuronal health in the adult L1 wing nerve might be impacted by loss of Ddr from glia. To test this, we labeled the ~40 glutamatergic neurons in the wing nerve using the *QF2/QUAS* binary system (*VGlut-QF2; QUAS-6xGFP*)(Potter et al., 2010), while at the same time using *Repo-Gal4* to

FIGURE 5

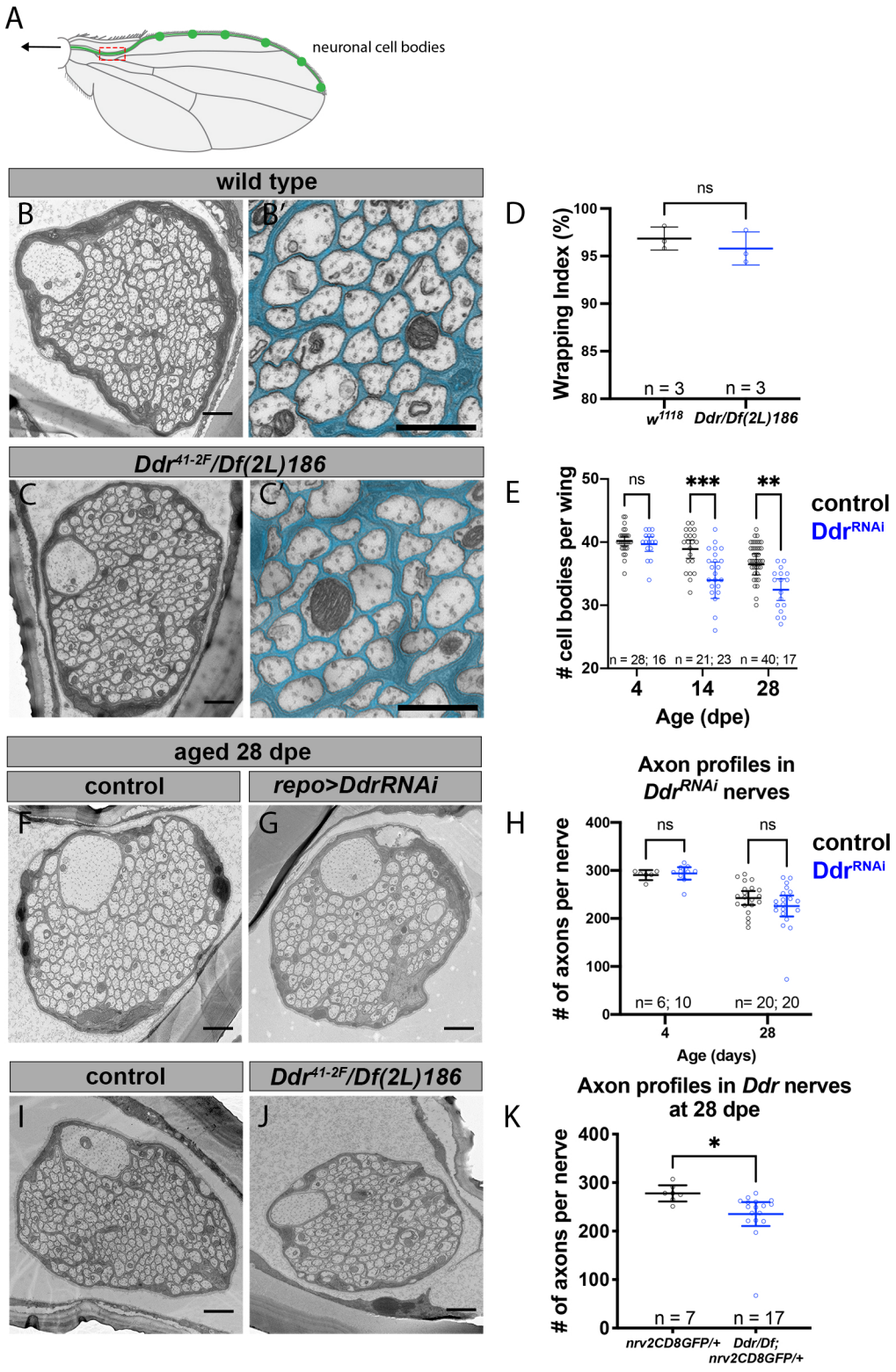

Figure 5: Loss of Ddr impairs long-term neuronal survival without affecting wrapping in adult nerves

(A) Schematic of the adult fly wing. The L1 vein lies along the anterior margin of the wing and contains ~280 sensory neuron cell bodies, a subset are depicted in green. The axons of these neurons coalesce to form the L1 sensory nerve which projects into the body towards the fly CNS. The TEM imaging window is shown in red. In this location axons from all of the L1 sensory neurons are present, allowing for quantifications. (*cont. next page*)

Figure 5 (cont.)
(B) Cross section TEM of the L1 nerve shows that axons are separated from each other by glial membranes by 5 dpe. (B') Magnified view from B with wrapping glia pseudocolored cyan. **(C)** Nerve morphology including wrapping is comparable in *Ddr* mutant nerves at this age, with axons separated and no obvious signs of impaired wrapping glia morphology. (C') Magnified view from C with wrapping glia pseudocolored cyan. **(D)** Wrapping index of *Ddr* loss of function animals is unchanged compared to control. (Unpaired t-test, p=0.4378) **(E)** There is a reduction in the number of healthy glutamatergic GFP+ cell bodies in wings from aged Ddr^{RNAi} knockdown animals compared to age-matched controls. (Two-way ANOVA with Sidak's multiple comparisons. 4dpe p=0.9774; 14dpe p=0.0007; 28dpe p=0.005) **(F)** Representative TEM image of a control nerve at 28 dpe shows normal wrapping/axon separation. **(G)** Representative Ddr^{RNAi} knockdown nerve at 28 dpe also shows normal wrapping/axon separation. A wrapping glia nucleus is present in this section (asterisk). **(H)** Quantification of axon profiles in 28 dpe control and *Ddr* mutant animals shows a modest but significant reduction in axons in *Ddr* as compared to controls. (Unpaired t-test, p=0.0343) **(I)** Representative TEM of a control nerve from a 28 dpe animal shows normal wrapping. **(J)** Representative TEM of a nerve from a 28 dpe *Ddr* mutant animal also shows normal wrapping. **(K)** Quantification of axon profile number in control and Ddr^{RNAi} glial knockdown nerves show no statistically significant difference in age dependent axon loss in contrast to our findings focusing on VGlut+ neuronal cell bodies by fluorescence (E). (Two-way ANOVA with Sidak's multiple comparisons; 4 dpe p=0.9755; 28 dpe p=0.2519)
Scale bars: B, C, F, G, I , J =1μm; B'& C' = 600nm

knockdown Ddr in glia using RNAi. We examined wings at 4, 14, or 28 **d**ays **p**ost **e**closion (dpe) and counted healthy GFP+ neuronal cell bodies along the wing margin at these timepoints from control and Ddr-RNAi animals to determine if loss of Ddr had any impact on long term neuronal survival. The number of neuronal cell bodies at 4 dpe was the same between control and *Ddr* knockdown animals suggesting that knockdown of *Ddr* did not affect neurogenesis (Figure 5B). Despite beginning with the same number of neurons (Figure 5E: 4 dpe mean cell body count = 40.2 vs. 39.7, p=0.9774), we found that there were significantly fewer healthy cell bodies in aged *Ddr-RNAi* wings compared to control at both ages examined (Figure 5E; 14 dpe mean cell body count 38.9 vs 34.0, p=0.0007; 28 dpe mean cell body count 36.5 vs 32.5, p=0.005, 2-way ANOVA with Sidak's multiple comparisons). These results indicate that despite not overtly disrupting glial ensheathment, knockdown of *Ddr* in glial cells negatively impacts long-term neuron health and survival.

To confirm and extend these findings we used TEM to visualize L1 nerves from aged control and glial *Ddr-RNAi* animals. We collected cross sections from a region in which all axons should be present so we could compare the total number of axon profiles within the nerve. To mirror our fluorescent experiments, we used the same genotypes and we first examined wings at 4 dpe. The number of axon profiles in control nerves at 4 dpe showed little variation and was indistinguishable from *Ddr-RNAi* (Figure 5H: mean axon profile count 290.3±10 vs 293.9±18.3, p=0.98). In aged (28 dpe) control and *Ddr* knockdown wing nerves, although wrapping again appeared normal, there was overall more variability in axon profile counts (Figure 5F-H: control= 242.7±31.02, *Ddr-RNAi* =226±46.5 axon profiles), but there was no significant difference in axon profile count in the *Ddr-RNAi* condition (Figure 5E-G; p=0.25, 2-way ANOVA with Sidak's multiple comparisons. This is in contrast to our findings in the same

genotype when we focused exclusively on *VGlut-QF2+* cell bodies (which marks ~40 cell bodies out of ~290 cell bodies total in the L1 nerve), We repeated these experiments using *Ddr* mutant animals and found a small but significant difference in the number of axon profiles (~15% fewer axons) consistent with the size of our original findings with fluorescent labeling of a subpopulation of these neurons (Figure 5I-K; control =277.9 ± 17.9, *Ddr* = 235.2 ± 48.2, p=0.022, unpaired t-test). Since the effect was stronger in whole animal mutants, this may reflect insufficient RNAi knockdown, but we cannot rule out that loss of Ddr from neurons, or another tissue might contribute to this effect, or that only specific subsets of neurons are particularly vulnerable to Ddr loss. Nevertheless, these data indicate that glial Ddr modulates the long-term health of sensory neurons.

Glial Ddr promotes increased axon caliber

Myelination can induce many changes in underlying axons including the redistribution of axonal proteins and increased axon caliber (Stassart et al., 2018), but whether non-myelinating ensheathment has similar effects is not known. One striking feature of the ultrastructure of the L1 wing nerve was the presence of a single, prominent, large caliber axon (Figure 5B). This axon is thus immediately identifiable in every sample, allowing us to directly compare its features across animals and conditions. A survey of the literature revealed that this axon likely belongs to the **d**istal **t**win **s**ensilla of the **m**argin (dTSM) neuron that innervates a campaniform sensillum (Dickinson and Palka, 1987). A striking but unexpected observation was that the dTSM axon in *Ddr* mutant and knockdown conditions was significantly smaller than in controls even though it was still clearly identifiable as the largest axon in the nerve. We quantified axon caliber by measuring the cross-sectional surface area of this uniquely identifiable axon and comparing

FIGURE 6

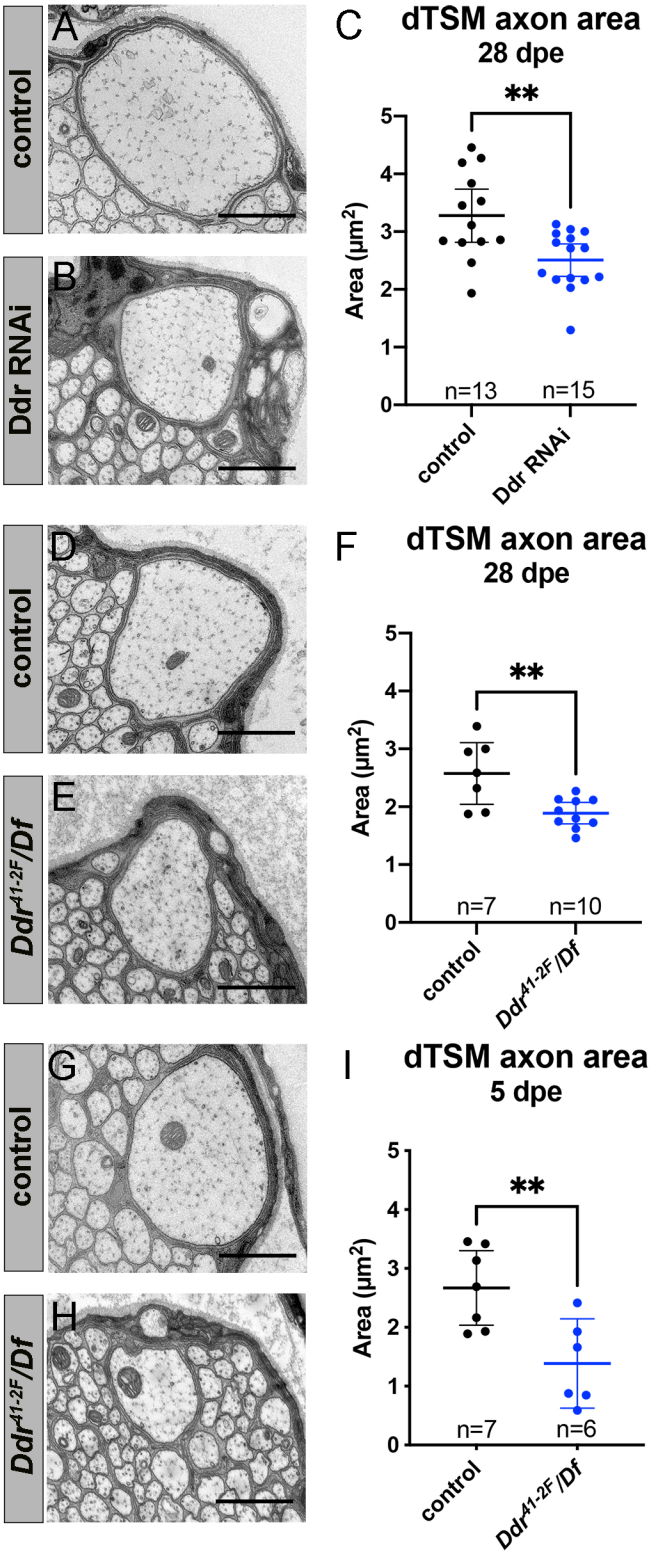

Figure 6: Ddr is required for normal axon caliber growth
(A-C) Axon caliber of the dTSM axons as measured by the cross-sectional area in TEM images is reduced in 28 dpe Ddr^{RNAi} nerves compared to age-matched controls. (Unpaired t-test; p=0.0037) **(D-F)** Axon caliber of the dTSM axons as measured by the cross sectional area in TEM images is reduced in 28 dpe *Ddr* loss of function nerves compared to age-matched controls. (Unpaired t-test; p=0.0044) **(G-I)** Axon caliber of the dTSM axons as measured by the cross sectional area in TEM images is already reduced in 5 dpe *Ddr* loss of function nerves compared to age-matched controls suggesting that initial axon maturation is perturbed when Ddr is absent. (Unpaired t-test; p=0.0073) Scale bars 1µm.

appropriate controls to *Ddr* mutant or glial *Ddr-RNAi* conditions from our 28 day aged wing TEM images. We found that in both glial-specific *Ddr*-knockdown and *Ddr* whole animal mutant nerves the caliber of the dTSM axon was significantly reduced compared to controls, revealing a role for glial Ddr in modulating axonal caliber (Figure 6A-F).

To determine whether reduced caliber is due to reduced growth versus shrinkage, we examined dTSM caliber in control and *Ddr* mutant wings from 5 dpe and found that the reduction in size is even greater at this age (Figure 6G-I). dTSM axon caliber is reduced by ~48% in *Ddr* mutants at 5 dpe (mean area: control = 2.670um^2 and *Ddr* = 1.387um^2) and ~27% at 28 dpe (mean area control = 2.575um^2 and *Ddr* = 1.890um^2). We have examined a small number of L1 nerves from wild type freshly eclosed flies (<24hours post eclosion) and observed that axons appear smaller than those from our standard 5 dpe timepoint suggesting that the first few days post eclosion are an important period of axon growth and maturation (Figure 6—figure supplement 1). Together these data suggest that the reduced caliber we see in *Ddr* mutants is due to impaired growth, rather than shrinkage. Since knockdown of Ddr selectively in glia is sufficient to cause a similar reduction in caliber to what is observed in whole animal mutants (~23% reduction at 28 dpe in RNAi experiments) our data identifies a cell non-autonomous role for glial Ddr in the control of axon caliber.

The reduced neuronal survival and decreased caliber we observed led us to wonder if we would observe any behavioral defects in adults as a result of Ddr loss. dTSM likely provides important proprioceptive feedback during flight, but its exact role in modifying flight behavior has not been established, making it difficult to directly test the effects of its reduced caliber on behavior. One well-established, testable behavior in adult flies is the escape reflex mediated by the giant fiber system. In this response, visual input activates the giant fiber neuron in the CNS,

which then activates an interneuron, that innervates a peripheral motor neuron to initiate a jump/escape response. This circuit is extremely fast and reliable. We reasoned that if the motor neuron axons in this circuit (the relevant peripheral axons in this circuit) were impaired in some way, there might be a measurable decrease in the muscle response probability after stimulation or an increased latency. We tested this reflex electrophysiologically in control and *Ddr* mutant animals but found no significant differences between the genotypes in either young or 28 dpe animals (Figure 6—figure supplement 2).

Ddr interacts with _Mp_ to promote wrapping in larval nerves

Our data indicate that Ddr performs essential roles in wrapping glia development and function. We next sought to understand the molecular mechanism(s) by which Ddr might mediate these functions. Mammalian Ddrs are activated by collagens *in vitro* and are thus considered non-canonical collagen receptors (Vogel et al., 1997). We wondered if *Drosophila* Ddr also interacts with collagen(s) to mediate its effects on wrapping in the larvae. The *Drosophila* genome contains 3 collagen genes. One of them, *Multiplexin* (*Mp*), was identified as a potential hit that affected wrapping glia morphology in third instar nerves in our initial screen. Knockdown of *Mp* using *nrv2-Gal4* caused moderate to severe wrapping defects when analyzed by confocal microscopy (Figure 7A-B). We studied expression of Mp protein in wild type nerves by using a MiMiC-GFP line in which the endogenous Mp protein is tagged with GFP. We observed punctate GFP expression throughout larval nerves suggesting that Mp, a secreted protein, is expressed by one or more of the cell types within the nerve (Figure 7C).

To determine whether *Ddr* and *Mp* might be working in the same genetic pathway to modulate wrapping in larval nerves, we crossed heterozygous *Ddr* and *Mp* mutants together and

FIGURE 7

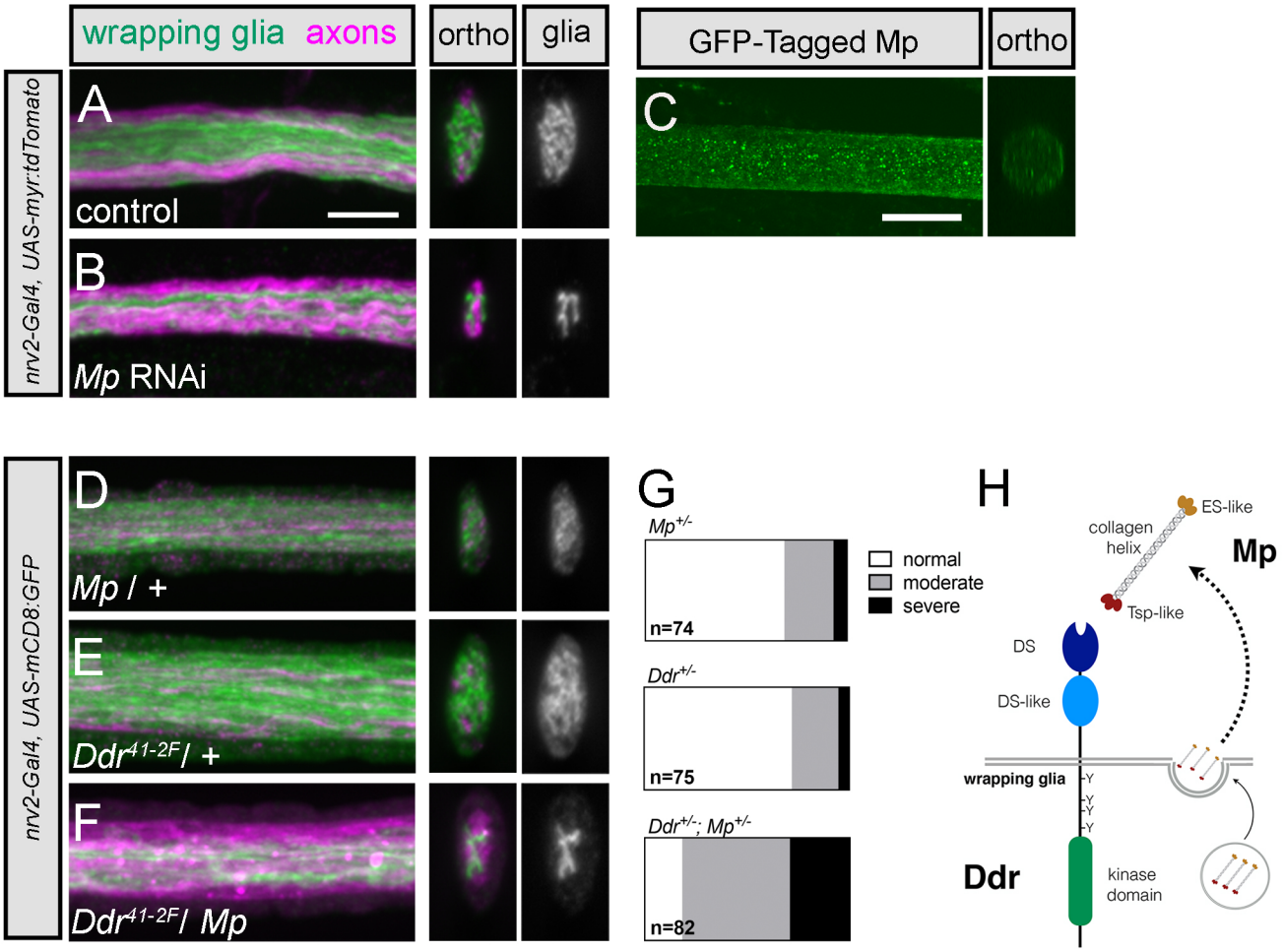

Figure 7: *Mp* genetically interacts with *Ddr* to promote wrapping in larval nerves

(A-B) Representative images of control and *Mp* RNAi knockdown in larval nerves. *Nrv2-Gal4* driven tdTomato is psuedocolored green. A subset of axons is labeled with anti-futsch antibody (magenta). Compared to control nerves, RNAi conditions show large areas of the nerve cross section without glia membrane coverage. **(C)** Mp-GFP expression in larval nerves. A MiMiC construct that adds a GFP tag to Mp protein is localized throughout larval nerves. **(D-F)** *Mp* and *Ddr* heterozygous nerves show normal wrapping glia morphology with good glial coverage of the nerve cross section indicating that one copy of each gene is sufficient to promote wrapping. In double heterozygous animals missing just one copy of each gene, however, coverage of the cross section is reduced indicating that wrapping is impaired. **(G)** Categorical scoring of *Ddr* and *Mp* single and double heterozygotes. n= # of nerves analyzed from 9-11 larvae per condition. **(H)** Proposed model of Mp and Ddr interaction. Based on the strong phenotype observed when Mp is knocked down specifically in wrapping glia, we hypothesize that wrapping glia secrete Mp which can act as autocrine activator of Ddr to drive normal wrapping glia morphogenesis.

356 analyzed the double heterozygous progeny for defects in larval wrapping glia morphology.
357 While animals that were heterozygous for either gene on its own did not show defects in
358 wrapping glia morphology, we found that the double heterozygous animals exhibited moderate
359 to severe defects in glial morphology (*Ddr/+*: 77% normal morphology; *Mp/+:* 72% normal
360 morphology; *Ddr/Mp*: 18% normal morphology; Figure 7D-G). These data suggest a strong
361 genetic interaction between the *Ddr* and *Mp* loci and imply they might function in a common
362 genetic pathway to control wrapping glia morphological development. Given that RNAi
363 knockdown of *Mp* specifically in wrapping glia is sufficient to cause a wrapping defect, our data
364 suggest a model in which Mp acts in an autocrine fashion to activate Ddr and drive downstream
365 signaling to promote wrapping (Figure 7H).
366
367 **Discussion**
368 Non-myelinating ensheathment of axons is a conserved but understudied feature of
369 peripheral nervous systems. Although this type of multi-axonal ensheathment has been less
370 studied as compared to myelination, a growing body of evidence indicates it is important for the
371 health and function of neurons and axons in the periphery. For example, Schwann cell specific
372 loss of the transmembrane receptor LDL receptor related protein-1 (LRP1) causes both thin
373 myelin and abnormal Remak bundle structure. These cKO animals also showed a lowered pain
374 threshold, suggesting that the physiology of nociceptor neurons is impaired when Remak
375 ensheathment is disrupted (Orita et al., 2013). Disrupting metabolism in SCs causes progressive
376 axon loss, with small unmyelinated fibers dying first, before myelinated fibers begin to show
377 signs of degeneration (Beirowski et al., 2014; Viader et al., 2013, 2011). In the fly, disruption of
378 axonal wrapping leads to uncoordinated behavioral responses that hint at aberrant ephaptic

379 coupling between neighboring axons in nerves when not properly separated (Kottmeier et al.,
380 2020). Such coupling could cause inappropriate activation of sensory or nociceptive neurons
381 underlying peripheral neuropathies. Previous studies from our lab have shown that wrapping glia
382 are required to clear neuronal debris after nerve injury and mediate injury signaling between
383 injured and intact "bystander" neurons which might be important for functional recovery after
384 nerve trauma (Hsu et al., 2021; Neukomm et al., 2014). These and other findings suggest that
385 Remak-type ensheathment and axon-glia signaling of unmyelinated fibers plays a variety of
386 underappreciated roles in peripheral nerve physiology that contribute to the pathophysiology of a
387 number of PNS disorders including debilitating peripheral neuropathies and responses to nerve
388 injury.

389 In order to gain insight into non-myelinating ensheathment, we used the *Drosophila*
390 peripheral nerves to identify a novel molecular pathway important for the development and
391 function multi-axonal ensheathment. We generated a new Split-Gal4 intersectional driver to
392 specifically target wrapping glia for functional and behavioral studies to better understand how
393 wrapping glia support axon health, physiology and ultimately circuit function. Finally, we
394 uncovered roles for glia in mediating long-term neuronal survival and driving increased axon
395 caliber that are separable from overt effects on wrapping, demonstrating that non-myelinating
396 ensheathing glia perform critical, previously unappreciated, roles in nervous system
397 development, maintenance, and function.

398

399 *Ddr and Mp regulate wrapping in larval nerves*

400 A main advantage of *Drosophila* is the ability to conduct large scale *in vivo* screens. We
401 made use of available *UAS-RNAi* libraries to broadly screen for novel regulators of axonal

ensheathment in intact nerves. Our morphological screen was sensitive enough to identify genes previously implicated in wrapping glia development including *vn*, *LamB1*, and *mys*, validating our approach. Moreover, in the case of *Ddr*, we were able to identify an important novel regulator of ensheathment that a simple behavioral or lethality screen would have missed in light of our follow-up behavioral testing. Knockdown of *Ddr* specifically in wrapping glia resulted in reduced glial membrane coverage in nerve cross sections by fluorescence microscopy. Similar phenotypes were observed in *Ddr* loss-of-function animals and could be rescued by resupplying Ddr specifically in wrapping glia, confirming the specificity of our RNAi results. TEM clearly showed that reduced glial membrane coverage at the light level corresponds to decreased axon wrapping. Unexpectedly, we observed that strong overexpression of *Ddr* using a *5XUAS-Ddr* construct in a control background caused frequent morphological defects in wrapping glia that were not observed when using a *1XUAS-Ddr* construct, suggesting that Ddr signaling must be tightly regulated to successfully promote wrapping.

Though neither of the vertebrate homologs, Ddr1 or Ddr2 has been explicitly implicated in glial development, several lines of evidence suggests that Ddr1 may have a conserved role in vertebrate glial development or function. Ddr1 is highly expressed in the mouse OL lineage starting from when the cells begin to associate with axons, is upregulated in newly formed OLs after cuprizone treatment, and is expressed in both myelinating and Remak Schwann cells (Franco-Pons et al., 2009, 2006; Gerber et al., 2021; Zhang et al., 2014). Moreover, Ddr1 is expressed in human oligodendrocytes and myelin, and variants in the human gene have been correlated with abnormal white matter and schizophrenia (Gas et al., 2018; Roig et al., 2010).

Vertebrate Ddr1 and Ddr2 are potently activated by collagens in vitro (Vogel et al., 1997), prompting us to investigate whether collagens were involved with Ddr function in fly

nerves. We had discovered that loss of the *Drosophila* collagen Mp disrupted glial morphology in our initial RNAi screening, and so investigated whether these genes might work together to promote ensheathment. Together with mammalian Ddrs established roles as collagen receptors, the strong genetic interaction we observed between *Ddr* and *Mp* is consistent with a model in which Mp acts as a collagen ligand for Ddr during axonal ensheathment. Our expression data from the *Mp-GFP* protein trap showed expression throughout the nerve. Although previous reports indicate that Mp is also expressed in one or both of the outer peripheral glia layers that extend beyond the nerve to cover NMJ synapses (Wang et al., 2019), the strong ensheathment defect seen when *Mp* is knocked down exclusively in wrapping glia indicates that wrapping glia themselves are the primary source of the Mp required for wrapping glia morphogenesis.

We hypothesize that Mp can act an autocrine collagen ligand to activate glial Ddr to drive wrapping in larval nerves (Figure 7H). This parallels developing Schwann cells, which secrete their own basal lamina, several components of which acts as regulators of their development including laminins and collagen. For example, laminin-211 serves as a ligand for GPR126 to promote myelination (Petersen et al., 2015). Mp is the sole *Drosophila* homolog of collagen types XV/XVIII, containing a central helical collagen region with a cleavable N-terminus thrombospondin like domain and C-terminal endostatin like domain (Meyer and Moussian, 2009; Myllyharju and Kivirikko, 2004). Collagen 15a1 and 18a1 are expressed in mouse peripheral nerves and *col15a1* mutants have radial sorting defects, suggesting that *Mp*'s role in promoting axon wrapping is likely conserved (Chen et al., 2015; Gerber et al., 2021; Rasi et al., 2010). In fact, *Mp* appears to play multiple important roles in nerve biology. Mp secreted by the outer glia layers acts via its cleaved endostatin domain, which is essential for homeostatic plasticity at motor neuron synapses (Wang et al., 2019, 2014). How Ddr activation within wrapping glia

ultimately drives axon wrapping still remains to be determined, but Ddr joins two other RTKs—EGFR and FGFR—as important and conserved regulators of axon ensheathment (Franzdóttir et al., 2009; Kottmeier et al., 2020; Matzat et al., 2015).

Wrapping glia are required for normal larval behavior

The *nrv2-Gal4* driver has been the standard method to genetically target wrapping glia in the field for many years but is imperfect for manipulation of wrapping glia in ablation or behavioral assays due to its expression in several subtypes of CNS glia. We generated a new Split-Gal4 intersectional driver that drives exclusively in wrapping glia. This allowed us to perform precise wrapping glia ablation. We found that genetic ablation of wrapping glia led to severely impaired larval locomotion, indicating the wrapping glia are essential for basic crawling circuit function. This phenotype was particularly striking in light of that fact that we did not observe any clear crawling defect in *Ddr* mutant larvae, even though wrapping was severely impaired. There are several possible explanations for these observations. First, it may be possible that non-contact mediated mechanisms, such as one or more secreted factors constitute wrapping glia's essential contribution to axon health and physiology. Alternatively, perhaps even a small amount of direct glia-axon contact at any point along the axon length may be sufficient to support axon function. This would be consistent with the lack of overt behavioral defects in newly-hatched 1st instar larvae, which have poor wrapping compared to later stages (Matzat et al., 2015; Stork et al., 2008), and even in wild type third instar larvae, in which not every axon is individually wrapped. This supports the notion that at least in the larvae, wrapping per se may not be strictly required, but glial presence and/or metabolic support and perhaps at least some contact is sufficient to support function for the ~5 days of larval life. Our results are similar to

what has been recently reported (Kottmeier et al., 2020) using a different approach to target wrapping glia for ablation, where only minor behavioral defects were observed when disrupting the FGFR signaling but profound crawling defects were seen upon ablation. Together these data support the conclusion that even limited wrapping or simply some degree of glia-axon contact is sufficient to support axon survival and nerve function compared to no glia at all.

Loss of Ddr impairs long-term neuronal survival

To better study the long-term functional effects of Ddr loss in wrapping glia, we turned to an adult nerve. Previous studies of oligodendrocytes and Schwann cells have found that impairing glial function can result in seemingly normal wrapping and circuit function in young animals, with deficits only appearing when the system is stressed or aged (Beirowski et al., 2014; Lappe-Siefke et al., 2003; Saab et al., 2016; Zöller et al., 2008), and studying wrapping in the adult allows for aging and maintenance studies that the short larval period precludes. Adult peripheral nerves are encased in a transparent but hard cuticle that allows for live-imaging but makes fixation challenging. Because of the resolution limits of light microscopy, we established a reliable method to study their ultrastructure using TEM. We found that the wrapping of axons by glia in the adult wing nerve is strikingly different from the larva, as all axons appear to be separated and individually ensheathed by glial membranes. To our surprise, wrapping was not obviously impaired in adult nerves of *Ddr* knockdown or mutant animals. Whether this is because it causes only a transient delay during pupal development, or is simply not required for adult wrapping glia morphogenesis remains unclear. In larval wrapping glia, there are 3 RTKs (EGFR, the FGFR heartless, and now Ddr) that are each required for normal ensheathment, and thus cannot fully compensate for one another (Kottmeier et al., 2020; Matzat et al., 2015). One

494 difference between larval and adult wrapping glia is the size of each cell. One larval wrapping
495 glia cell covers the majority of the nerve length from where it exits the VNC to the territory of
496 the second wrapping glia which has its cell body where nerve enters the muscle field. This means
497 that the wrapping glia cell must undergo tremendous growth to both keep up with longitudinal
498 growth as the animal grows and elongates the nerve, as well as radial growth to separate axons.
499 A single cell can end up covering from ~750um-2.5mm of nerve length depending on the
500 segment. In the wing nerve, there are ~15 wrapping glia along the region of the L1 nerve we
501 analyze, which is ~400um long. Perhaps in the larval system the cell is pushed to its growth
502 limits and any perturbation in pro-wrapping signaling has a strong effect of morphology, whereas
503 in the adult nerve the system is robust and redundant enough to withstand perturbations of single
504 genes.

505 Despite no obvious wrapping effect, however, we found that loss of *Ddr* did affect the
506 sensory neurons in the nerve as animals naturally aged. The uncoupling of neuron health from
507 overt effects on myelination has been demonstrated previously. For example, *Cnp1* mutant mice
508 show severe age-dependent neurodegeneration although they have grossly normal myelin with
509 only subtle changes in myelin ultrastructure revealed by special fixation techniques (Lappe-
510 Siefke et al., 2003; Snaidero et al., 2017). Similarly, loss of PLP results in axon degeneration
511 despite having normal myelin with only subtle ultrastructural defects (Garbern et al., 2002;
512 Griffiths et al., 1998; Klugmann et al., 1997). We found that the number of VGlut+ neurons was
513 reduced in aged wings of *Ddr* knock down animals, indicating that glial *Ddr* is important for
514 long-term neuronal survival. When we analyzed *Ddr* whole animal mutants by TEM we found a
515 small but significant reduction in axon profile number, which should correspond to the number
516 of living neurons. The effects were modest, and together with the increased variability observed

suggests to us that absence of Ddr signaling increases the susceptibility of subpopulations of neurons to insult or injury that may underlie age-related degeneration rather than outright causing them to die. While we cannot rule out the possibility that loss of Ddr from neurons or epithelial cells contributes to the effect we see in the whole animal mutant experiments, taken together our data support a role for Ddr in mediating axon-glia signaling that contributes to the long-term health of peripheral neurons.

Glial Ddr regulates axon caliber

Myelination can directly affect the structure and function of the axons they wrap, including controlling caliber. In general, myelination increases caliber. For example, dysmyelinated *Trembler* mice have reduced axon calibers compared to controls (Waegh et al., 1992) and in the PNS caliber along a single axon can vary with reduced caliber at points without direct myelin contact, such as nodes of Ranvier (Hsieh et al., 1994). Axon caliber is an important determinant of conduction velocity but varies widely between neuronal subtypes, so achieving and maintaining appropriate caliber for each axon during development is likely to be critical for proper circuit function. How non-myelinating ensheathment might impact axon caliber has not been as clearly established. Here, we find that glial Ddr promotes increased axon caliber of a non-myelinated axon. We focused on the dTSM axon, which can be reliably identified across animals, so we could directly compare caliber between conditions. The reductions we observed in axon caliber were similar between *Ddr* mutants and when Ddr was specifically lost from glia cells, supporting a non-cell autonomous role for glial Ddr in regulating axon caliber. The effect is considerable—nearly a 50% reduction in axon caliber at 5 dpe. We hypothesize that by this

time point, wildtype dTSM axons have reached their mature caliber, as it is comparable between 5 dpe and 28 dpe in comparable genetic backgrounds. In *Ddr* mutants, however, we observe that the relative size compared to controls changes over time, suggesting that in *Ddr* mutants (or knockdowns) the axon continues to increase its caliber, perhaps in an effort to achieve the optimal size, though the axons still remain ~25% smaller than wild type axons at 28 dpe.

Two proteins, MAG, which acts to increase caliber of myelinated axons (Yin et al., 1998), and CMTM6, which restricts caliber of myelinated and unmyelinated axons (Eichel et al., 2020) are the only proteins reported to cell non-autonomously affect caliber of vertebrate axons. In the fly, a shift in the average size of axons in larval nerves is observed when wrapping glia are absent or severely disrupted supporting a general role for wrapping in promoting axon size (Kottmeier et al., 2020). Interestingly, we show that Ddr is required for increased axon caliber even when wrapping appears intact supporting a direct role for glial Ddr in promoting increased caliber. The exact molecular mechanism by which Ddr may promote increased caliber size remains unclear. The control of axon caliber, generally, is not well understood, with few studies looking at either cell autonomous or non-autonomous control of caliber. Genes involved in the general regulation of cell size have been implicated as cell autonomous determinants. For example, in the fly, S6 kinase signaling is a positive regulator of motorneuron size, including axon caliber, though the exact mechanisms that determine final caliber remain unknown (Cheng et al., 2011). In mammalian axons, it is believed that the phosphorylation state of neurofilaments and microtubules ultimately determines their spacing to control caliber (Yin et al., 1998). It seems unlikely that *glial* Ddr can directly phosphorylate *axonal* microtubules, so determining how Ddr activity in glia influences the axonal cytoskeleton to control caliber growth is an important next step. Our giant fiber assay did not reveal any clear deficits in escape reflex

562 circuitry, but this circuitry mediates an extremely robust all-or-none escape response that does
563 not depend on proprioceptive feedback along long peripherally wrapped axons. A 25-50%
564 reduction in caliber would be predicted to impact conduction velocity along the dTSM axon and
565 given that campaniform sensilla provide essential rapid sensory feedback to fine tune movement,
566 it will be of interest to test conduction velocity and/or flight behavior directly in *Ddr* mutant
567 animals to see how the proprioceptive circuit might be affected.

568 Taken together, our studies identify Ddr an an important regulator of wrapping glia
569 development and function in the fly, with distinct roles in larval and adult wrapping glia. Ddr is
570 essential for the normal morphological development of axon wrapping in the larvae, and later it
571 mediates important axon-glia communication that controls axon caliber growth and affects
572 neuronal health and survival. Given its expression pattern in vertebrate oligodendrocytes and
573 Schwann cells, it seems likely that one or more of these essential functions is conserved in
574 vertebrates. Further study into how Ddr functions in both fly and vertebrate glia promises to
575 increase our understanding of axon ensheathment in health and disease.

576

577 **Methods**

578 ***Drosophila* genetics**

579 *Drosophila melanogaster* were raised according to standard laboratory conditions. Larval
580 RNAi experiments, including controls, were conducted at 29°C to increase expression of the
581 UAS-RNAi constructs. All other experimental crosses and aging experiments were conducted at
582 25°C. A full list of all fly strains used in this study can be found as a table in the Supplemental

583 Methods. Fly strains generated for this study include *Ddr*$^{41\text{-}2F}$, *Ddr*$^{13\text{-}1M}$, *WG-SplitGal4, 5XUAS-*
584 *Ddr* and *1XUAS-Ddr.* Full details on their construction are also in the Supplemental Methods.
585
586 **Immunohistochemistry and Confocal Analysis**
587 For confocal fluorescent imaging, larvae were filleted on sylgard plates in room
588 temperature (RT) PBS and fixed on a shaker in 4% paraformaldehyde (Electron Microscopy
589 Sciences, EMS) in PBS for 20 minutes. After washing with PBS and PBST (0.3% Triton-X),
590 larvae were incubated in primary antibodies overnight at 4°C with gentle agitation on a shaker.
591 After washing in PBST at RT on a shaker, secondary antibodies were added and incubated
592 overnight at 4°C on a shaker, shielded from light. After washes in PBST, samples were mounted
593 on glass slides using Vectashield (Vector Labs). The following primary antibodies were used in
594 this study: chicken α-GFP (1:1000, Abcam, ab13970); rabbit α-DsRed (1:600, Clontech,
595 #632496); rat α-mCherry (1:2000, Invitrogen, #16D7); mouse α-futsch (22C10, 1:500, DSHB);
596 mouse α-Repo (1:100, DSHB); goat α-HRP pre-conjugated to Alexa488, CY3, or CY5 (1:100,
597 Jackson Immuno Research); rabbit α-Oaz (1:5000, this study, see details below). Primary
598 antibodies were detected with the appropriate donkey secondary antibody conjugated to DyLight
599 488, Alexa488, Cy3, Rhodamine Red-X, CY5, or DyLight 405 reconstituted per the
600 manufacturer's instructions and use at final dilutions of 1:250 (Jackson Immuno Research).
601 Phalloidin-iFluor 647 and 405 were used at 1:2500 (Abcam).
602 Confocal images were obtained on either an Innovative Imaging Innovations (3i)
603 spinning-disk confocal microscope equipped with a Yokogawa CSX-X1 scan head and
604 Hamamatsu camera with SlideBook software (3i) or on a Zeiss spinning disk confocal
605 microscope equipped with a Yokogawa CSX-X1 scan head and Hamamatsu camera with Zen

606 software. Images were obtained with 10x air, 40x 1.3NA Oil, or 63x 1.4NA Oil objectives.
607 Confocal stacks taken to analyze wrapping glia morphology in nerve cross sections were taken
608 with the 63x objective, using the recommended optimal slice size of 0.27 microns.
609 To score wrapping glia morphology, images were obtained from regions ~200 microns
610 from the tip of the VNC (to roughly correspond to the TEM analysis location). At 63x
611 magnification ~100um of nerve length could be analyzed in an image. Orthogonal sections were
612 visualized using SlideBook or Zen software and the cross section of each nerve was examined
613 over the length in the captured image. Morphology was scored categorically as being "normal,"
614 having "moderate" defects in nerve coverage, or having "severe" defects in nerve coverage.
615 Nerves were not scored if the Z axis of a particular nerve was too compressed to visualize
616 morphology well. Representative orthogonal views were exported to prepare figures. See Figure
617 2—figure supplement 1 for images and descriptions of each category. The number of larvae and
618 nerves scored for each quantified genotype is included in the text or appropriate Figure legend.
619

620 **Electron microscopy**

621 Third instar larvae were manually processed for TEM as dissected fillets, using standard
622 TEM processing procedures. Drosophila wings were processed using microwave-assisted
623 fixation with a protocol adapted from (Cunningham and Monk, 2018; Czopka and Lyons, 2011)
624 protocols for zebrafish larvae, with the main differences being the elimination of all 10 minute
625 RT "hold" steps. After fixation and embedding in Embed-812, 70nm sections were collected on
626 200 mesh copper grids (larvae) or 100 mesh Formvar film coated grids (wings), counterstained
627 with UA and lead citrate and imaged on a Tecnai T12 electron microscope operating at 80kV or

120kV accelerating voltage equipped with an AMT digital camera and software. Full details of fixation and processing are available in the Supplemental Methods.

Aging assay and live imaging of wings

Animals of appropriate genotypes were crossed at 25°C. Correct progeny were selected using visible markers and aged in small groups in cornmeal agar vials for the indicated number of days at 25°C. Flies were transferred to fresh food vials every 3-7 days. On the appropriate day (4, 14, or 28 days after collection), flies were anesthetized and one wing was removed from each animal using fine dissection scissors (Fine Science Tools). Wings used for fluorescence imaging were mounted in Halocarbon oil 27 (Sigma) on glass slides for live imaging as described in (Neukomm et al., 2014). For the neuronal survival assay, wings were inspected for tears and injuries along the L1 vein at 63x with transmitted light and only wings with no visible physical damage were assessed further. GFP+ cell bodies were visualized and counted using a Zeiss Spinning Disk confocal system (Axio Examiner equipped with a Yokogawa spinning disk, Hamatsu camera, and Zen software) using a 63xNA1.4 oil objective. Cells were counted as intact if they had a clear nucleus and dendrite or were considered dead if they were shrunken and the dendrite or nucleus were not clearly visible. Wings to be analyzed by TEM were immediately placed in fixative and processed as described in the Supplemental Methods.

Larval Tracking

Larval crawling behavior was analyzed using the frustrated total internal reflection imaging method and FIMTrack software (Risse et al., 2017). Briefly, larvae were washed briefly in ddH20 and kept on agar plates prior to testing. Approximately 5 larvae of the same genotype

651 were placed near the center of a 0.8% agar surface positioned above an IR camera using a
652 paintbrush. Behavior was recorded at RT at 10 frames/second for 1 minute. Videos were
653 analyzed using FIMTrack software to extract data about individual larva. Crawling paths for
654 each larva were automatically generated by FIMTrack and information of total distance travelled
655 for each larva was exported to Excel and converted from pixels to cm before being analyzed
656 using GraphPad PRISM software. Only larvae that were successfully tracked for the full minute
657 were included in the analysis.
658
659 **Giant Fiber Assay**
660 This assay was performed essentially as described in (Allen and Godenschwege, 2010).
661 Flies of the appropriate genotype and age are mounted ventral side down under a microscope.
662 Stimulating electrodes were placed through the eyes to the brain and a recording electrode was
663 placed in the DLM muscle. 100 or 200 Hz stimulation trains were applied and responses were
664 recorded in the DLM muscle. The number of responses and the latency of the first response were
665 quantified. Data were analyzed with the GraphPad Prism, using either Mann-Whitney's test (for
666 non-parametric data) or Welch's t-test (for parametric data) to determine statistical differences.
667
668 **Analysis and Statistics**
669 TEM image analysis was performed in FIJI/ImageJ using an AMT plugin to import
670 image metadata. Wrapping index (WI) was quantified as described in Matzat et al, 2015.
671 Briefly, the Cell Counter plugin was used to manually tally the total number of axons and then
672 manually tally the number of bundles or singly wrapped axons. WI was then computed for each
673 nerve as: # of singly wrapped + # axon bundles/Total # of axons, expressed as a percentage.

Axon counts in wing nerves were also performed manually with the Cell Counter plugin in FIJI. dTSM cross sectional area was performed using the polygon selection tool to manually trace the circumference of the dTSM axon and then using the Measure Tool to obtain the cross-sectional area that had been outlined. Nerves were excluded from an analysis if knife marks, resin folds, or debris blocked the feature(s) needing to be measured or if the section angle was too far from perpendicular resulting in elongated and blurry axonal profiles. For larval experiments, both male and female larvae were used unless the genetics of a specific experiment only allowed for one sex to be used (e.g. transgene on the X chromosome coming from a male parent). For adult experiments only female flies (wings) were used. Wing size and the number and type of sensory neruons present in the wing are sexually dimorphic, which necessitated using a single sex to compare axon number and caliber. Females were selected because their wings are slightly larger and thus easier to handle, and this facilitates genetic experiments that involve genes and/or transgenes on the X chromosome.

Statistical analysis was performed using GraphPad Prism software. The appropriate statistical test was determined based on the experimental design and how many conditions were being compared. Details on the exact sample sizes and statistical tests used are included in the corresponding Results section and/or Figure.

Author Contributions:

M.M.C.: Conceptualization, Methodology, Formal Analysis, Investigation, Data Curation, Writing-Original Draft, Visualization, Project Administration, Funding Acquisition

A.P.L.: Methodology, Formal Analysis, Investigation, Data curation, Writing-Review and Editing, Visualization
J.Q.H.: Methodology, Investigation, Writing-Review and editing
A.E.S.: Investigation
F.J.B-G.: Investigation, Formal Analysis, Writing-Review and Editing, Visualization
G. W.D.: Resources, Writing-Review and Editing, Funding Acquistion
S.A.A.: Resources, Writing-Review and Editing, Funding Acquisition
M.R.F.: Conceptualization, Resources, Generation of the anti-Oaz antibody, Writing-Review and Editing, Project Administration, Supervision, Funding Acquisition

Acknowledgements

We are grateful to Dr. Christian Klambt, Dr. Joshua Dubnau, the Bloomington Stock Center, and the Vienna Drosophila Resource Center for providing fly stocks. We would like to acknowledge FlyBase.org for being an invaluable research tool for *Drosophila* scientists (Larkin et al., 2020). Anti-futsch (22C10), anti-Repo (8D12), and anti-Elav (7E8A10) monoclonal antibodies developed by Drs. Seymor Benzer, Corey Goodman, & Gerald Rubin (respectively) were obtained from the Developmental Studies Hybridoma Bank created by the NICHD of the NIH and maintained at The University of Iowa, Department of Biology, Iowa City, IA 52242. We thank Dr. Michael Brodsky for assistance with CRISPR-Cas9 mediated mutagenesis. We thank Dr. Lara Strittmatter and the staff of the University of Massachusetts Medical Center Electron Microscopy Facility; Dr. Robert Kayton and Dr. Lisa Vecchiarelli of the OHSU Electron Microcopy Facility; and Dr. Deborah Hegarty for their expertise and assistance with TEM protocol development and equipment. We are indebted to Dr. Kelly Monk and the Monk lab for TEM advice and generous sharing of their microwave tissue processing equipment. We thank Rachel Bradshaw for her help with the RNAi screen and Alex Larson for her assistance with TEM prep work. Finally, we thank all members of the Freeman lab for their advice and feedback throughout this project. This work was supported by NINDS P30 NS061800 (SAA) and NINDS R01NS112215 & R01059991(MRF). MRF was an investigator with the Howard Hughes Medical Institute during a portion of this study.

729 References

730
731

732 Allen MJ, Godenschwege TA. 2010. Electrophysiological Recordings from the Drosophila Giant
733 Fiber System (GFS). *Cold Spring Harb Protoc* 2010:pdb.prot5453. doi:10.1101/pdb.prot5453

734 Barros CS, Nguyen T, Spencer KSR, Nishiyama A, Colognato H, Müller U. 2009. Beta1
735 integrins are required for normal CNS myelination and promote AKT-dependent myelin
736 outgrowth. *Development (Cambridge, England)* 136:2717–2724. doi:10.1242/dev.038679

737 Beirowski B, Babetto E, Golden JP, Chen Y-J, Yang K, Gross RW, Patti GJ, Milbrandt J. 2014.
738 Metabolic regulator LKB1 is crucial for Schwann cell-mediated axon maintenance. *Nature*
739 *neuroscience* 1–15. doi:10.1038/nn.3809

740 Chen P, Cescon M, Bonaldo P. 2015. The Role of Collagens in Peripheral Nerve Myelination
741 and Function. *Molecular neurobiology* 52:216–225. doi:10.1007/s12035-014-8862-y

742 Cheng L, Locke C, Davis GW. 2011. S6 kinase localizes to the presynaptic active zone and
743 functions with PDK1 to control synapse development. *J Cell Biology* 194:921–935.
744 doi:10.1083/jcb.201101042

745 Coutinho-Budd JC, Sheehan AE, Freeman MR. 2017. The secreted neurotrophin Spätzle 3
746 promotes glial morphogenesis and supports neuronal survival and function. *Gene Dev*
747 31:2023–2038. doi:10.1101/gad.305888.117

748 Cunningham RL, Monk KR. 2018. Schwann Cells, Methods and Protocols 385–400.
749 doi:10.1007/978-1-4939-7649-2_26

750 Czopka T, Lyons DA. 2011. Chapter 2 Dissecting Mechanisms of Myelinated Axon Formation
751 Using Zebrafish. *Methods Cell Biol* 105:25–62. doi:10.1016/b978-0-12-381320-6.00002-3

752 Dickinson M, Palka J. 1987. Physiological properties, time of development, and central
753 projection are correlated in the wing mechanoreceptors of Drosophila. *J Neurosci* 7:4201–
754 4208. doi:10.1523/jneurosci.07-12-04201.1987

755 Eichel MA, Gargareta V-I, D'Este E, Fledrich R, Kungl T, Buscham TJ, Lüders KA, Miracle C,
756 Jung RB, Distler U, Kusch K, Möbius W, Hülsmann S, Tenzer S, Nave K-A, Werner HB.
757 2020. CMTM6 expressed on the adaxonal Schwann cell surface restricts axonal diameters in
758 peripheral nerves. *Nat Commun* 11:4514. doi:10.1038/s41467-020-18172-7

759 Feltri ML, Porta DG, Previtali SC, Nodari A, Migliavacca B, Cassetti A, Littlewood-Evans A,
760 Reichardt LF, Messing A, Quattrini A, Mueller U, Wrabetz L. 2002. Conditional disruption of
761 beta 1 integrin in Schwann cells impedes interactions with axons. *The Journal of cell biology*
762 156:199–209. doi:10.1083/jcb.200109021

763 Franco-Pons N, Tomàs J, Roig B, Auladell C, Martorell L, Vilella E. 2009. Discoidin domain
764 receptor 1, a tyrosine kinase receptor, is upregulated in an experimental model of
765 remyelination and during oligodendrocyte differentiation in vitro. *Journal of molecular*
766 *neuroscience : MN* 38:2–11. doi:10.1007/s12031-008-9151-x

767 Franco-Pons N, Virgos C, Vogel WF, Ureña JM, Soriano E, Rio JA del, Vilella E. 2006.
768 Expression of discoidin domain receptor 1 during mouse brain development follows the
769 progress of myelination. *Neuroscience* 140:463–475. doi:10.1016/j.neuroscience.2006.02.033

770 Franzdóttir SR, Engelen D, Yuva-Aydemir Y, Schmidt I, Aho A, Klämbt C. 2009. Switch in
771 FGF signalling initiates glial differentiation in the Drosophila eye. *Nature* 460:758–761.
772 doi:10.1038/nature08167

773 Furusho M, Dupree JL, Bryant M, Bansal R. 2009. Disruption of fibroblast growth factor
774 receptor signaling in nonmyelinating Schwann cells causes sensory axonal neuropathy and
775 impairment of thermal pain sensitivity. *The Journal of neuroscience : the official journal of*
776 *the Society for Neuroscience* 29:1608–1614. doi:10.1523/jneurosci.5615-08.2009

777 Garbern JY, Yool DA, Moore GJ, Wilds IB, Faulk MW, Klugmann M, Nave K, Sistermans EA,
778 Knaap MS van der, Bird TD, Shy ME, Kamholz JA, Griffiths IR. 2002. Patients lacking the
779 major CNS myelin protein, proteolipid protein 1, develop length-dependent axonal
780 degeneration in the absence of demyelination and inflammation. *Brain* 125:551–561.
781 doi:10.1093/brain/awf043

782 Gas C, Canales-Rodríguez EJ, Radua J, Abasolo N, Cortés MJ, Salvadó E, Muntané G, Alemán-
783 Gómez Y, Julià T, Marsal S, Sanjuan J, Guitart M, Costas J, Martorell L, Pomarol-Clotet E,
784 Vilella E. 2018. Discoidin domain receptor 1 gene variants are associated with decreased
785 white matter fractional anisotropy and decreased processing speed in schizophrenia. *J*
786 *Psychiatr Res* 110:74–82. doi:10.1016/j.jpsychires.2018.12.021

787 Gerber D, Pereira JA, Gerber J, Tan G, Dimitrieva S, Yángüez E, Suter U. 2021. Transcriptional
788 profiling of mouse peripheral nerves to the single-cell level to build a sciatic nerve ATlas
789 (SNAT). *Elife* 10:e58591. doi:10.7554/elife.58591

790 Ghosh A, Kling T, Snaidero N, Sampaio JL, Shevchenko A, Gras H, Geurten B, Göpfert MC,
791 Schulz JB, Voigt A, Simons M, Perrimon N. 2013. A Global In Vivo Drosophila RNAi
792 Screen Identifies a Key Role of Ceramide Phosphoethanolamine for Glial Ensheathment of
793 Axons. *PLoS genetics* 9:e1003980. doi:10.1371/journal.pgen.1003980.s012

794 Gohl DM, Silies MA, Gao XJ, Bhalerao S, Luongo FJ, Lin C-C, Potter CJ, Clandinin TR. 2011.
795 A versatile in vivo system for directed dissection of gene expression patterns. *Nature methods*
796 8:231–237.

797 Griffin JW, Thompson WJ. 2008. Biology and pathology of nonmyelinating Schwann cells. *Glia*
798 56:1518–1531. doi:10.1002/glia.20778

799 Griffiths I, Klugmann M, Anderson T, Yool D, Thomson C, Schwab MH, Schneider A,
800 Zimmermann F, McCulloch M, Nadon N, Nave KA. 1998. Axonal swellings and
801 degeneration in mice lacking the major proteolipid of myelin. *Science (New York, NY)*
802 280:1610–1613.

803 Hilchen CM von, Bustos AE, Giangrande A, Technau GM, Altenhein B. 2013. Predetermined
804 embryonic glial cells form the distinct glial sheaths of the Drosophila peripheral nervous
805 system. *Development (Cambridge, England)*. doi:10.1242/dev.093245

806 Hsieh S, Kidd G, Crawford T, Xu Z, Lin W, Trapp B, Cleveland D, Griffin J. 1994. Regional
807 modulation of neurofilament organization by myelination in normal axons. *J Neurosci*
808 14:6392–6401. doi:10.1523/jneurosci.14-11-06392.1994

809 Hsu J-M, Kang Y, Corty MM, Mathieson D, Peters OM, Freeman MR. 2021. Injury-Induced
810 Inhibition of Bystander Neurons Requires dSarm and Signaling from Glia. *Neuron* 109:473-
811 487.e5. doi:10.1016/j.neuron.2020.11.012

812 Klugmann M, Schwab MH, Pühlhofer A, Schneider A, Zimmermann F, Griffiths IR, Nave K-A.
813 1997. Assembly of CNS Myelin in the Absence of Proteolipid Protein. *Neuron* 18:59–70.
814 doi:10.1016/s0896-6273(01)80046-5

815 Kottmeier R, Bittern J, Schoofs A, Scheiwe F, Matzat T, Pankratz M, Klämbt C. 2020. Wrapping
816 glia regulates neuronal signaling speed and precision in the peripheral nervous system of
817 Drosophila. *Nat Commun* 11:4491. doi:10.1038/s41467-020-18291-1

818 Lappe-Siefke C, Goebbels S, Gravel M, Nicksch E, Lee J, Braun PE, Griffiths IR, Nave K-A.
819 2003. Disruption of Cnp1 uncouples oligodendroglial functions in axonal support and
820 myelination. *Nature genetics* 33:366–374. doi:10.1038/ng1095

821 Larkin A, Marygold SJ, Antonazzo G, Attrill H, dos Santos G, Garapati PV, Goodman JL,
822 Gramates LS, Millburn G, Strelets VB, Tabone CJ, Thurmond J, Consortium F, Perrimon N,
823 Gelbart SR, Agapite J, Broll K, Crosby M, Santos G dos, Falls K, Gramates LS, Jenkins V,
824 Longden I, Matthews B, Sutherland C, Tabone CJ, Zhou P, Zytkovicz M, Brown N,
825 Antonazzo G, Attrill H, Garapati P, Larkin A, Marygold S, McLachlan A, Millburn G,
826 Pilgrim C, Ozturk-Colak A, Trovisco V, Kaufman T, Calvi B, Goodman J, Strelets V,
827 Thurmond J, Cripps R, Lovato T. 2020. FlyBase: updates to the Drosophila melanogaster
828 knowledge base. *Nucleic Acids Res* 49:D899–D907. doi:10.1093/nar/gkaa1026

829 Luan H, Peabody NC, Vinson CR, White BH. 2006. Refined spatial manipulation of neuronal
830 function by combinatorial restriction of transgene expression. *Neuron* 52:425–436.
831 doi:10.1016/j.neuron.2006.08.028

832 Lyons DA, Pogoda H-M, Voas MG, Woods IG, Diamond B, Nix R, Arana N, Jacobs J, Talbot
833 WS. 2005. erbb3 and erbb2 are essential for schwann cell migration and myelination in
834 zebrafish. *Current biology : CB* 15:513–524. doi:10.1016/j.cub.2005.02.030

835 Matzat T, Sieglitz F, Kottmeier R, Babatz F, Engelen D, Klämbt C. 2015. Axonal wrapping in
836 the Drosophila PNS is controlled by glia-derived neuregulin homolog Vein. *Development*
837 *(Cambridge, England)* 142:1336–1345. doi:10.1242/dev.116616

838 Meyer F, Moussian B. 2009. Drosophila multiplexin (Dmp) modulates motor axon pathfinding
839 accuracy. *Development, growth & differentiation* 51:483–498. doi:10.1111/j.1440-
840 169x.2009.01111.x

841 Michailov GV, Sereda MW, Brinkmann BG, Fischer TM, Haug B, Birchmeier C, Role L, Lai C,
842 Schwab MH, Nave K-A. 2004. Axonal Neuregulin-1 Regulates Myelin Sheath Thickness.
843 *Science* 304:700–703. doi:10.1126/science.1095862

844 Monk KR, Feltri ML, Taveggia C. 2015. New insights on schwann cell development. *Glia*.
845 doi:10.1002/glia.22852

846 Mukherjee C, Kling T, Russo B, Miebach K, Kess E, Schifferer M, Pedro LD, Weikert U, Fard
847 MK, Kannaiyan N, Rossner M, Aicher M-L, Goebbels S, Nave K-A, Krämer-Albers E-M,
848 Schneider A, Simons M. 2020. Oligodendrocytes Provide Antioxidant Defense Function for
849 Neurons by Secreting Ferritin Heavy Chain. *Cell Metab* 32:259-272.e10.
850 doi:10.1016/j.cmet.2020.05.019

851 Myllyharju J, Kivirikko KI. 2004. Collagens, modifying enzymes and their mutations in humans,
852 flies and worms. *Trends Genet* 20:33–43. doi:10.1016/j.tig.2003.11.004

853 Nave K-A. 2010. Myelination and support of axonal integrity by glia. *Nature* 468:244–252.
854 doi:10.1038/nature09614

855 Neukomm LJ, Burdett TC, Gonzalez MA, Züchner S, Freeman MR. 2014. Rapid in vivo forward
856 genetic approach for identifying axon death genes in Drosophila. *Proceedings of the National*
857 *Academy of Sciences* 111:9965–9970. doi:10.1073/pnas.1406230111

858 Ochoa J, Mair WG. 1969. The normal sural nerve in man. I. Ultrastructure and numbers of fibres
859 and cells. *Acta neuropathologica* 13:197–216.

860 Orita S, Henry K, Mantuano E, Yamauchi K, Corato AD, Ishikawa T, Feltri ML, Wrabetz L,
861 Gaultier A, Pollack M, Ellisman M, Takahashi K, Gonias SL, Campana WM. 2013. Schwann
862 cell LRP1 regulates remak bundle ultrastructure and axonal interactions to prevent
863 neuropathic pain. *The Journal of neuroscience : the official journal of the Society for*
864 *Neuroscience* 33:5590–5602. doi:10.1523/jneurosci.3342-12.2013

865 Pereira JA, Benninger Y, Baumann R, Gonçalves AF, Ozçelik M, Thurnherr T, Tricaud N,
866 Meijer D, Fässler R, Suter U, Relvas JB. 2009. Integrin-linked kinase is required for radial
867 sorting of axons and Schwann cell remyelination in the peripheral nervous system. *The*
868 *Journal of cell biology* 185:147–161. doi:10.1083/jcb.200809008

869 Petersen SC, Luo R, Liebscher I, Giera S, Jeong S-J, Mogha A, Ghidinelli M, Feltri ML,
870 Schöneberg T, Piao X, Monk KR. 2015. The adhesion GPCR GPR126 has distinct, domain-
871 dependent functions in Schwann cell development mediated by interaction with laminin-211.
872 *Neuron* 85:755–769. doi:10.1016/j.neuron.2014.12.057

873 Petley-Ragan LM, Ardiel EL, Rankin CH, Auld VJ. 2016. Accumulation of Laminin Monomers
874 in Drosophila Glia Leads to Glial Endoplasmic Reticulum Stress and Disrupted Larval
875 Locomotion. *Journal of Neuroscience* 36:1151–1164. doi:10.1523/jneurosci.1797-15.2016

876 Potter CJ, Tasic B, Russler EV, Liang L, Luo L. 2010. The Q system: a repressible binary system
877 for transgene expression, lineage tracing, and mosaic analysis. *Cell* 141:536–548.
878 doi:10.1016/j.cell.2010.02.025

879 Rasi K, Hurskainen M, Kallio M, Stavén S, Sormunen R, Heape AM, Avila RL, Kirschner D,
880 Muona A, Tolonen U, Tanila H, Huhtala P, Soininen R, Pihlajaniemi T. 2010. Lack of
881 collagen XV impairs peripheral nerve maturation and, when combined with laminin-411
882 deficiency, leads to basement membrane abnormalities and sensorimotor dysfunction. *The*
883 *Journal of neuroscience : the official journal of the Society for Neuroscience* 30:14490–
884 14501. doi:10.1523/jneurosci.2644-10.2010

885 Risse B, Berh D, Otto N, Klämbt C, Jiang X. 2017. FIMTrack: An open source tracking and
886 locomotion analysis software for small animals. *PLoS computational biology* 13:e1005530.
887 doi:10.1371/journal.pcbi.1005530

888 Roig B, Franco-Pons N, Martorell L, Tomàs J, Vogel WF, Vilella E. 2010. Expression of the
889 tyrosine kinase discoidin domain receptor 1 (DDR1) in human central nervous system myelin.
890 *Brain research* 1336:22–29. doi:10.1016/j.brainres.2010.03.099

891 Saab AS, Tzvetavona ID, Trevisiol A, Baltan S, Dibaj P, Kusch K, Möbius W, Goetze B, Jahn
892 HM, Huang W, Steffens H, Schomburg ED, Pérez-Samartín A, Pérez-Cerdá F, Bakhtiari D,
893 Matute C, Löwel S, Griesinger C, Hirrlinger J, Kirchhoff F, Nave K-A. 2016.
894 Oligodendroglial NMDA Receptors Regulate Glucose Import and Axonal Energy
895 Metabolism. *Neuron* 91:119–132. doi:10.1016/j.neuron.2016.05.016

896 Schmalbruch H. 1986. Fiber composition of the rat sciatic nerve. *The Anatomical record* 215:71–
897 81. doi:10.1002/ar.1092150111

898 Snaidero N, Velte C, Myllykoski M, Raasakka A, Ignatev A, Werner HB, Erwig MS, Möbius W,
899 Kursula P, Nave K-A, Simons M. 2017. Antagonistic Functions of MBP and CNP Establish
900 Cytosolic Channels in CNS Myelin. *Cell Reports* 18:314–323.
901 doi:10.1016/j.celrep.2016.12.053

902 Stassart RM, Fledrich R, Velanac V, Brinkmann BG, Schwab MH, Meijer D, Sereda MW, Nave
903 K-A. 2013. A role for Schwann cell-derived neuregulin-1 in remyelination. *Nature*
904 *neuroscience* 16:48–54. doi:10.1038/nn.3281

905 Stassart RM, Möbius W, Nave K-A, Edgar JM. 2018. The Axon-Myelin Unit in Development
906 and Degenerative Disease. *Front Neurosci-switz* 12:467. doi:10.3389/fnins.2018.00467

907 Stork T, Engelen D, Krudewig A, Silies M, Bainton RJ, Klämbt C. 2008. Organization and
908 function of the blood-brain barrier in Drosophila. *The Journal of neuroscience : the official*
909 *journal of the Society for Neuroscience* 28:587–597. doi:10.1523/jneurosci.4367-07.2008

910 Taveggia C, Zanazzi G, Petrylak A, Yano H, Rosenbluth J, Einheber S, Xu X, Esper RM, Loeb
911 JA, Shrager P, Chao MV, Falls DL, Role L, Salzer JL. 2005. Neuregulin-1 type III determines
912 the ensheathment fate of axons. *Neuron* 47:681–694. doi:10.1016/j.neuron.2005.08.017

913 Viader A, Golden JP, Baloh RH, Schmidt RE, Hunter DA, Milbrandt J. 2011. Schwann Cell
914 Mitochondrial Metabolism Supports Long-Term Axonal Survival and Peripheral Nerve
915 Function. *J Neurosci* 31:10128–10140. doi:10.1523/jneurosci.0884-11.2011

916 Viader A, Sasaki Y, Kim S, Strickland A, Workman CS, Yang K, Gross RW, Milbrandt J. 2013.
917 Aberrant Schwann cell lipid metabolism linked to mitochondrial deficits leads to axon
918 degeneration and neuropathy. *Neuron* 77:886–898. doi:10.1016/j.neuron.2013.01.012

919 Vogel W, Gish GD, Alves F, Pawson T. 1997. The discoidin domain receptor tyrosine kinases
920 are activated by collagen. *Molecular cell* 1:13–23.

921 Waegh SM de, Lee VM-Y, Brady ST. 1992. Local modulation of neurofilament
922 phosphorylation, axonal caliber, and slow axonal transport by myelinating Schwann cells.
923 *Cell* 68:451–463. doi:10.1016/0092-8674(92)90183-d

924 Wang T, Hauswirth AG, Tong A, Dickman DK, Davis GW. 2014. Endostatin Is a Trans-
925 Synaptic Signal for Homeostatic Synaptic Plasticity. *Neuron* 83:616–629.
926 doi:10.1016/j.neuron.2014.07.003

927 Wang T, Morency DT, Harris N, Davis GW. 2019. Epigenetic Signaling in Glia Controls
928 Presynaptic Homeostatic Plasticity. *Neuron* 105:491-505.e3.
929 doi:10.1016/j.neuron.2019.10.041

930 Xie X, Auld VJ. 2011. Integrins are necessary for the development and maintenance of the glial
931 layers in the Drosophila peripheral nerve. *Development (Cambridge, England)* 138:3813–
932 3822. doi:10.1242/dev.064816

933 Yin X, Crawford TO, Griffin JW, Tu P h, Lee VM, Li C, Roder J, Trapp BD. 1998. Myelin-
934 associated glycoprotein is a myelin signal that modulates the caliber of myelinated axons. *J*
935 *Neurosci* 18:1953–1962. doi:10.1523/jneurosci.18-06-01953.1998

936 Yu W-M, Yu H, Chen Z-L, Strickland S. 2009. Disruption of laminin in the peripheral nervous
937 system impedes nonmyelinating Schwann cell development and impairs nociceptive sensory
938 function. *Glia* 57:850–859. doi:10.1002/glia.20811

939 Zhang Y, Chen K, Sloan SA, Bennett ML, Scholze AR, O'Keeffe S, Phatnani HP, Guarnieri P,
940 Caneda C, Ruderisch N, Deng S, Liddelow SA, Zhang C, Daneman R, Maniatis T, Barres
941 BA, Wu JQ. 2014. An RNA-Sequencing Transcriptome and Splicing Database of Glia,
942 Neurons, and Vascular Cells of the Cerebral Cortex. *The Journal of neuroscience : the official*
943 *journal of the Society for Neuroscience* 34:11929–11947. doi:10.1523/jneurosci.1860-
944 14.2014

945 Zöller I, Meixner M, Hartmann D, Büssow H, Meyer R, Gieselmann V, Eckhardt M. 2008.
946 Absence of 2-Hydroxylated Sphingolipids Is Compatible with Normal Neural Development
947 But Causes Late-Onset Axon and Myelin Sheath Degeneration. *J Neurosci* 28:9741–9754.
948 doi:10.1523/jneurosci.0458-08.2008

949